# I. MAGNETOMETER SURVEY OF THE LA VENTA PYRAMID, 1969

Frank Morrison, C. W. Clewlow, Jr. and Robert F. Heizer

## Introduction

The La Venta pyramid, although the largest single structure at the important Olmec ceremonial center in lowland Tabasco, has until recently been afforded scant attention by researchers at the site. Early investigations there by Matthew Stirling and Philip Drucker were concentrated on the unique art style embodied in the large carved stone monuments and the problems of ceramic stratigraphy (cf. Stirling, 1943; Drucker, 1952). The large scale explorations of Drucker and Heizer in 1955 explored the complexities of Complex A (Drucker, Heizer, and Squier, 1959; Drucker and Heizer, 1965). Although the northern two-thirds of the site was mapped in 1955, the pyramid (referred to as Complex C) was covered with a dense growth of jungle cover and was incorrectly shown by the party surveyor to be a somewhat elongated rectangle.

It was with understandable surprise, then, that Drucker and Heizer viewed the pyramid in 1967, stripped of its heavy cover of foliage, and recognized that it was not rectangular at all, but was actually a fluted cone or, more technically, a conoidal frustum (Heizer and Drucker, 1968; Heizer, 1968). Ten alternating valleys and ridges were seen to run up the sloping surface of the structure's 100 foot elevation, spaced at roughly equal intervals around its circular basal plan. In 1968 Heizer returned to La Venta with a University of California field party and, among other things, completed a detailed topographic map, shown here in Figure 4, of the entire pyramid structure which constitutes Complex C (Heizer, Drucker, and Graham, 1968; Heizer, Graham, and Napton, 1968).

This entirely new information, as well as providing fresh insights into Olmec culture history (cf. Ibid., p. 137; Heizer, 1968, pp. 12-21), has generated a renewed interest in the unique structure itself (Bernal, 1969, pp. 35-36). Much of this interest of course revolves around the problems of the possible function of the mound and the possibilities that it might contain smaller buried structures. It was in hopes of providing partial answers to these questions that the 1969 magnetometer survey was conceived. It was known that most of the large Olmec carved monuments as well as the natural basalt columns which were used in the enclosure and the "tomb" in Complex A were of a highly magnetic basalt from the Tuxtla Mountains, some 70 kilometers to the west (Williams and Heizer, 1965). Samples of clays from the site constructions were tested and found to be effectively non-magnetic. Thus it was felt that should the Olmecs have buried any large stone monuments or built any structures of basalt within the pyramid they would be detected by a sensitive magnetometer (cf. Stuart and Stuart, 1969, p. 200).

Most of the groundwork for the survey was done in Berkeley by Heizer, who was unable to accompany the field party. The National Geographic Society through its Committee on Research and Exploration granted funds for the magnetometer survey. The authors wish to thank Dr. Melvin Payne, President of the NGS and Dr. Leonard Carmichael, Secretary of the Committee on Research and Exploration and the several members of the Committee for their support. The field party itself was led by F. Morrison of the Department of Materials Science and Engineering, University of California, Berkeley. He was aided by Jack Mego, an electronics technician in the same department, and by C. W. Clewlow, a graduate student in Anthropology. Invaluable assistance in Mexico City, in Villahermosa, and at the La Venta site itself was provided by Arql. Eduardo Contreras, Jr. of INAH, and Arql. Carlos Sebastian Hernandez, Conservador of the Museo del Estado, Villahermosa, Tabasco. Considerable enthusiasm and support from the Instituto Nacional de Antropologia e Historia through the Director, Dr. Ignacio Bernal, contributed immensely to the success of the survey. The survey itself took place between May 11 and May 29, 1969.

## Description of the Magnetometer

Calculations of the magnetic anomalies to be expected from significant basalt monuments buried within the La Venta pyramid were carried out on the computer at Berkeley prior to the field work. Samples of sand and clay from 1968 test excavations in the La Venta area were tested for magnetic susceptibility and found to be essentially non-magnetic. Assuming that the pyramid itself was constructed of similar materials, and consequently possessing no magnetic anomaly of its own, models consisting of basalt cubes three meters on a side were run on the computer and values of the anomalous magnetic field to be expected on the surface of an idealized model of the pyramid were obtained. These calculations indicated that to detect such a basalt structure, at the center and base of the pyramid, sensitivities as high as 0.05 gammas ($\gamma$) would be required (the Earth's total magnetic field at La Venta is approximately 43,000 $\gamma$). These same calculations showed that a station spacing of three meters would be adequate to detect any major structures.

Since natural time variations with periods from 1 second to diurnal are a characteristic of the Earth's magnetic field and because these time varying fields can have amplitudes from 0.01$\gamma$ to 100$\gamma$ (respectively) it is necessary to have a means of correcting for, or eliminating, these variations in order to conduct such a high sensitivity magnetometer survey. The time varying magnetic field is uniform over distances measured in kilometers so that an obvious solution for small area surveys is to use two magnetometers and measure the difference in the field. In this way, if one magnetometer is placed in a fixed position the roving magnetometer will map the field due to subsurface effects independently of the time variations. This configuration was selected for the La Venta survey.

An alternate procedure which is often used in conventional geophysical prospecting is to use only one sensor and to return periodically to a fixed point, correcting the intervening readings in proportion to the amount the

field at the fixed point has varied. This method is inappropriate if sensitivities of 1.0γ or less are required because it would be necessary to reoccupy the fixed station every 15 to 20 seconds.

The two-sensor difference magnetometer is useful for high sensitivity surveys only if each sensor is itself of high sensitivity and consequently such surveys have been possible only since the development of the alkali vapour magnetometer. These devices have limiting sensitivities of 0.001γ and operating sensitivities of 0.01γ are easy to achieve. The first two-sensor difference survey, using Varian rubidium vapour magnetometers, was conducted in 1965 (Breiner, 1965, Rainey and Ralph, 1966), and in the summer of 1966 two fully developed systems were used with great success in the search for Sybaris (Ralph, Morrison and O'Brien, 1968). A more complete description of the operation of the alkali vapour magnetometers may be found in the articles referenced above.

To describe the actual electronics associated with the measurement of the fields, it is only necessary to note that the output from an alkali vapour magnetometer is a frequency proportional to the magnetic field in which the sensor is placed. In the case of the rubidium sensor, the constant of proportionality is 4.667 cycles per second per gamma (Hz/ γ). Thus in a field of 40,000γ the frequency output of the magnetometer would be 186,680 Hz. For cesium the constant is 3.499 Hz/γ. These output frequencies are easily measured on standard electronic counters (devices to measure the number of cycles in a prescribed time). We can now easily determine the sensitivity of a single magnetometer; for rubidium a change of 1γ in the field changes the frequency by 4.667 Hz. If the counter displays the integer number of cycles in one second, we have a sensitivity of ±1 cycle/second or approximately 1/4.667γ. If we count for 10 seconds, we then have a sensitivity of 0.1 cycle/second or approximately 1/46.67γ.

Ideally in difference operation we would use a counter that measured the difference in two output frequencies. The Varian portable magnetometer readout unit accomplished this, but a simple and less expensive alternate approach is to use the configuration of Figure 1. This particular difference magnetometer used two different Varian sensors, one rubidium and one cesium. This was dictated solely by availability of sensors and in no way affects the theory of operation.

The entire magnetometer system was powered by a lightweight 350 watt gasoline motor-generator. Battery operation is also possible, but the weight of the batteries required for 8 hours of operation is as great as the generator plus gasoline. Moreover most electronic counters, especially those available on a rental basis, are 110v ac and would require an inverter for battery operation. This would simply replace the converter used in this system to supply the dc power to the sensors. The couplers associated with each sensor in Figure 1 are mixers that supply the regulated 28v dc power to the sensor and extract the output signal frequency returned from the sensor to be fed to the counter. In the Varian readout unit the two couplers, the power supply, and the counter are combined in a single unit powered by a battery pack.

We shall see below that it is not necessary to use a counter that actually measures the difference of the two sensor outputs. In fact, for "small" differences in magnetic field between the two sensors the ratio of the two frequency outputs is linearly proportional to the difference. This allows us to use any counter which can measure ratios. The Hewlett-Packard Model 5325Awas selected for this survey for its light weight, low power consumption and low monthly rental.

## Magnetometer Sensitivity

To show the relationship of ratio to difference for this magnetometer and to determine the difference mode sensitivity for the La Venta survey, the following calculations are included in this report.

Let the output frequency of the rubidium magnetometer be A Hz at a fixed point. At the same point the output of the cesium magnetometer will be B Hz. If the Earth's field at that point is Tγ , then A = 4.667T and B = 3.499T. The ratio A/B is 1.333809. [A more correct ratio, using more significant digits is 1.333400. This value thus constitutes the zero contour in this survey.]

Now, disregarding time variations for the moment, if the cesium magnetometer is moved to a position where the field has increased a small amount, δ , then the frequency output will increase δ × 3.499 or Δ . The ratio is now $A/(B+\Delta)$ or $A/B(1+\frac{\Delta}{B})$. Now if $\Delta/B << 1$, $(1 + \Delta/B)^{-1}$ may be expanded as $1 - \Delta/B + \Delta^2/B^2 - \ldots$ If $\Delta/B$ is less than .001, then neglecting the terms beyond $\Delta/B$ in the series will affect the value of $(1 - \Delta/B)^{-1}$ by less than one part in $10^6$. In that case the ratio becomes

$$\frac{A}{B} \left(1 - \frac{\Delta}{B}\right)$$

or

$$\frac{A}{B} - \frac{A}{B^2} \cdot \Delta$$

Thus, the ratio is a linear function of Δ.

We may now apply numbers from the La Venta survey. The mean value for A at La Venta was 202,700 Hz or 43,432.6γ. Thus the value of B is 202,700 × 3.499/4.667 or 151,970 so that $A/B^2$ becomes $8.77 \times 10^{-6}$. If the field at sensor B now increases by δγ's, then Δ = 3.499δ and the ratio becomes

$$\frac{A}{B} - 8.77 \times 10^{-6} \times 3.499\delta$$

or $1.333808 - 30.686 \times 10^{-6}$.

To translate this into limiting sensitivities, if we can measure the ratio to $\pm$ 1 unit in the sixth decimal place then the difference sensitivity is 1/30.6$\overline{86}$ or .0325$\gamma$/ unit. For six decimal ratio accuracy the count time was 1 second with the corresponding sensitivity of 0.325$\gamma$ . The entire survey at La Venta was conducted with a sensitivity of $\pm$ 0.0325$\gamma$. In retrospect, we will see below an order of magnitude less would have been satisfactory.

For this linear relationship between ratio and difference to hold it is only required that $\Delta/B$ be less than .001, ie., $3.499\delta/151{,}970$ be less than .001 or that $\delta$ be less than 43$\gamma$ approximately. Rarely do anomalies in excess of 100$\gamma$ occur in archaeological prospecting so it is seen that the magnetometer used here is, to a very high order, a true difference magnetometer. Practically speaking, if the anomaly is greater than 43$\gamma$ a sensitivity of $\pm$ 1 in the sixth decimal place of the ratio is unnecessary. With a relaxing of the sensitivity to $\pm$ 1 in the fifth place, the linear approximation is again valid for anomalies up to several hundred gammas.

There remains the proof that the time variations are in fact cancelled in such a configuration. We will consider the two outputs as before except that now the field increases by $\delta$ $\gamma$'s at each of them. The ratio then becomes

$$\frac{A + 4.667\delta}{B + 3.499\delta} \quad \text{or for convenience} \quad \frac{A + C_A\delta}{B + C_B\delta}$$

Note that $C_B/C_A = r$ a fixed constant. We may now write the ratio as

$$\frac{A\left[\,1 + \dfrac{C_A\delta}{A}\,\right]}{B\left[\,1 + \dfrac{C_B\delta}{B}\,\right]}$$

Again, if $C_B\delta/B$ is $<<1$, we may write this ratio as

$$\frac{A}{B}\left(1 + \frac{C_A\delta}{A}\right)\left(1 - \frac{C_B\delta}{B}\right)$$

$$= \frac{A}{B}\left(1 - \frac{C_B\delta}{B} + \frac{C_A\delta}{A} - \frac{C_AC_B\delta^2}{AB}\right)$$

Now

$$\frac{C_B}{B} = \frac{C_A}{A} = \frac{1}{T} \quad \text{so the two middle terms cancel leaving}$$

$$\frac{A}{B}\left(1 - \frac{\delta^2}{T^2}\right)$$

Here again we find that the restriction required to keep the ratio constant to 1 part in $10^6$ is that $\delta^2/T^2$ must be less than $10^{-6}$ approximately. At La Venta T is 43,000$\gamma$ so $\delta$ must be less than 43$\gamma$ .

Thus we find that for time variations to have no effect on the sixth decimal place of the ratio, the magnitude of the variation must be less than 43 $\gamma$. Since the normal short period variations that we are trying to eliminate are rarely greater than 10, we see that for all practical purposes the time variations will have no effect on the ratio. If variations greater than 43$\gamma$ do occur, they may be corrected for by monitoring the total field of the fixed sensor. Readings of total field frequency were recorded at half hour intervals during the survey to ensure that the amplitude did not change greatly. Maximum changes of less than 20$\gamma$ were common to all the data recording periods.

As indicated in Figure 1, the rubidium sensor was used as the fixed sensor and the cesium as the roving or mobile sensor. The technical reason for this choice is that the cesium sensor is less subject to orientation error and consequently easier to use as a hand carried device. It should be noted that the output frequency is independent of the orientation of the cell but that the signal-to-noise ratio is highest when the sensor axis is at 45° to the total-field direction and decreases away from this position--the decrease being less for cesium than for rubidium.

A final point is that this magnetometer provides an absolute zero for a particular area which is of some help in the interpretation of the data.

## Field Operation at La Venta

The equipment involved in the La Venta survey, schematically described in Figure 1, is shown packaged in Plate 1. In operation the fixed sensor was placed well away from the readout area and both it and the roving sensor were connected by coaxial cable to the readout unit. The fixed sensor and the roving sensor are shown together in Plate 2. The readout unit consisting of the two couplers, the power supply, and the counter is shown in Plates 3 and 4.

To facilitate carrying the roving sensor dragging its cable along with it, it was necessary to clear the pyramid of the dense underbrush (see Plate 5). Survey lines were then laid out radially using ordinary cord marked off in 3 meter intervals. Readings were taken each 3 meters out one line (Plate 7), the line was then swung approximately 6 meters in chord distance at the 60 meter radius and surveyed again. Intermediate values, between lines, at large radii were filled in by estimating position.

Azimuth readings were taken periodically and topographic features were noted on the survey lines so that the data could later be fitted accurately to the plan map of the pyramid. This surveying technique

was rather crude but relative positioning error is less than one meter and the maximum absolute error is less than 2 meters in the azimuthal direction and less than 1 meter in the radial direction. More accurate surveying procedures would have increased the survey time unreasonably without significant improvement in the overall data.

The ratio values at each station were recorded directly on radially scaled graph paper, an example of which is shown in Figure 2. This allowed preliminary contouring of data in the field as the example indicates. Note that the ratio values are inverted with respect to the true magnetic anomalies; that is, ratio lows correspond to magnetic highs and vice versa.

To facilitate steady positioning of the roving sensor on the often uneven surface of the pyramid the operator was "lowered" down the pyramid by a rope as shown in Plate 6. The process was found to be considerably easier on the sensor operator, inasmuch as scrambling up and down a 30° slope in high temperature and humidity can be rather wearying. The sensor was carried at a mean height of .8 meters above the ground.

All the equipment performed excellently. In the peak of the mid-day heat, the heater control unit in the rubidium sensor failed but this problem was easily eliminated by removing the unit. Apparently the high ambient temperature was sufficient to keep the cesium cell vaporized. The survey was completed in 8 days, and the equipment was actually on for a total of 41 hours. The progress of the survey was impeded in the early days by the fact that the pyramid could not be cleared fast enough by a work crew of eight men. The number was eventually increased to 24 and the survey progressed more rapidly. Further, due to encroaching houses with their associated debris, garden plots, etc., it was not possible to extend the survey radially as far as had been planned. This was extremely unfortunate because on most lines it was not possible to survey far enough away from the pyramid to get a zero or background reading, nor was it possible to search for any monuments, structures, etc., that might be near the base. Approximately 2500 data points were obtained.

## Data Processing

The field data were transferred to a large scale plan map of the pyramid and replotted. The ratio 1.334000 was chosen as the base for this plot and subtracted from all the readings. The readings were then contoured in levels of 100 units or 3.25$\gamma$. An ink tracing of the resulting contour map was then made with the contours now marked in (3.00$\gamma$ was assumed instead of the correct 3.25) and with the correct sign. This map was then photo-reduced to the same scale as the topographic map of the pyramid. This final contoured magnetic map is shown in Figure 3. The topographic map is shown in Figure 4. Finally, since shading or coloring of contour intervals emphasizes patterns not immediately evident from the contours, the map was then color shaded as shown in Figure 6.

The data were also converted to digital form for a later, more extended analysis by digital computer. A preliminary step in this analysis is the presentation of the magnetic data in a perspective view drawing. Like the color shading mentioned above these perspective drawings are helpful in discerning anomaly patterns that are difficult to recognize in the contour maps themselves. In Figure 3a a perspective view of the magnetic data, taken from the South East, is shown to illustrate this effect.

All the maps presented in this report are oriented with respect to magnetic north, since this is the important direction used in the interpretation.

## Interpretation

The color shaded map, Figure 6, shows the important magnetic patterns more clearly than the simple contoured map, Figure 3. The general pattern is one of strong radial anomalies on the southern half of the pyramid's surface, turning into gentle broad circumferencial anomalies on the northern half. Near the top and to the south is a striking magnetic high falling off sharply to the north into a tight arc-shaped low area. These anomalies show up clearly in the perspective view, Figure 3a. The major anomaly near the top is very evident in this persepctive view and stands out as the most important feature in the data. The color shading is likely to place undesirable emphasis on minor features if they happen to be colored overly brightly. Unfortunately this is the case for the blue areas of Figure 6. The eye is drawn to the blue as an area of maximum anomaly, whereas in fact it is only the small area of dark blue-violet near the top which is indicative of a truly anomalous region. The red area is clearly anomalous, sitting two full color intervals (orange and yellow) above the general "background". In interpreting the field map, it is also important to realize that the zero level contour is somewhat arbitrary. For the detailed analysis to follow, we have used the ratio value 1.334400, the approximate value of the rubidium/cesium constant, as the zero level but since this ratio will go up or down with respect to the fixed station it is obvious, for example, that if the fixed station were placed on the highest magnetic anomaly then the whole map would come out with negative contours. A better approach would be to take the mean of all the data points as a zero but this is a rather tedious process without having the data in digital form.

In the present case the choice of the zero level was somewhat subjective, having been arrived at after considerable experimentation with various models. We will see in the discussion to follow that it is the pattern of the interpretational model that is important rather than the exact numerical fit. The area at the top of the pyramid was not surveyed due to the presence of several concrete blocks with imbedded iron bolts. Some readings taken within 6 meters of the center showed steep gradients with anomalies as high as 100$\gamma$'s. It is unlikely, however, that the iron bolts are responsible for the extreme values of the magnetic low encountered about 6 meters due south of the center (the deep blue-violet on the color map)

and it is evident that the accentuation of the low at this point is due to very shallow magnetic objects, perhaps buried iron pipe.

The large magnetic low in the north west is caused by roofing metal, and probably a host of other iron objects associated with the closest of all the encroaching houses mentioned earlier.

The radial pattern is produced by the radial ridge and gully topography of the pyramid (see Figure 4). The Earth's magnetic field in the La Venta area has an inclination of approximately 45° so that on the north side of the pyramid the field is parallel to and inclined at only 15° to the ridge and gully pattern. At such low inclination very little secondary field is to be expected. On the eastern and western flanks, however, we might assume that the ridges were represented by long cylinders with a component of the field perpendicular to them, giving rise to typical high on the south low on the north anomalies. While the actual combination of multiple ridge effects will not yield a simple pattern the radial nature of the anomalies should be most pronounced on these flanks. On the southern surface the field is of high inclination to the ridges and of zero strike with respect to them, so that the pattern of the anomalies will be broad highs coinciding with the ridges. This general pattern is so well demonstrated in the magnetic map that there is little doubt that these features are in fact due to the topography.

The magnetic low area just off the centerline at the extreme south of the area surveyed coincides with a bulldozed excavation and probably results from the removal of this magnetic soil layer. A "hole" in magnetic material produces a reversed anomaly, i.e., a low over the hole surrounded by smaller highs. The pits on the north slope of the pyramid will have much smaller anomalies due to the low inclination of the field. The small anomaly almost on the center line at the southern margin of the map is a clear example of the inverse anomaly having been observed over a well defined pit about 1.5 m in diameter and 1.0 m deep. The small isolated 6$\gamma$ low about 15 m farther west is associated with a small basalt block of .5 m maximum dimension. The maximum anomaly expected from such a small block of basalt (susceptibility $10^{-3}$ e.m.u.) is on the order of 10$\gamma$. The interesting feature is, however, that the anomaly is negative rather than positive indicating a high magnetic remanence for the block. This fact will be considered further in the final summary.

The apparent high susceptibility of the soils was unanticipated, since soil samples from the La Venta site, taken in 1968, were tested for their magnetic susceptibility prior to the survey and found to be essentially non-magnetic. A crude test of soil susceptibility on the pyramid was made by placing small cups of soil of known volume four inches from the sensor. The highest anomaly produced in this test was .26$\gamma$, yielding a susceptibility of $7 \times 10^{-5}$ e.m.u. The uncertainty in this crude test is on the order of $5 \times 10^{-5}$ e.m.u. so it may only be concluded that the soil susceptibility is between $10^{-5}$ and $10^{-4}$ e.m.u. A too hasty calculation in the field led the senior author to believe the susceptibility was less than $10^{-5}$ and to conclude that the topographic effect was caused by a magnetic sub-layer.

Soil susceptibilities of this order are not uncommon. Le Borgne (1955), Aitken (1961), and Cook and Carts (1962) have shown that many highly organic soils have volume susceptibilities of $5 \times 10^{-4}$ e.m.u. due to the in-situ formation of the mineral maghemite. However, as Le Borgne has pointed out, in areas of high humidity where the drainage is sufficient, the iron is usually leached out. Why the soil of the La Venta pyramid should remain so magnetic is not known.

The contradiction between this survey's results and the tests made prior to the survey may be due to the following two factors. The "soil" samples tested may have been taken below the actual soil line or the pyramid may be made of quite different clays and sands than the surrounding features.

It should be noted for future work of this sort that the optimum survey should be preceded by some carefully controlled soil sampling and magnetic susceptibility measurements with a standard susceptibility bridge or with an in-situ susceptibility meter.

The effect of this surface layer of magnetic material is to mask anomalies from subsurface bodies with a "noise" level of 5 - 10γ. This could be removed by digital processing of the data, namely by assuming a surface layer of variable thickness and magnetic susceptibility and calculating, by surface integration for each data point, a new map of topographic anomalies alone. The best fit to the observed topographic effects would then be subtracted from the actual data leaving a map of anomalies from subsurface bodies. Fortunately in our case the main anomaly, just south of center, is sufficiently above the topographic noise level so that this costly correction is not necessary. In our discussion of this anomaly we will have occasion to discuss the effect of the topography on the interpretation, but it will not be necessary to make calculations for it.

Finally the presence of the pronounced topographic effect decreases the sensitivity requirement so that a sensitivity of 0.3γ would have been sufficient for this survey. This, however, could not have been foretold and the survey was actually run at a .0325γ sensitivity.

The large magnetic anomaly to the south of the center of the pyramid has been replotted in greater detail in the detail map, Figure 5. For this plot the ratio 1.334400 was chosen as the zero level, the ratios were converted accurately to gammas, and the final map was contoured with an interval of 2γ.

The pattern of this anomaly is complex, although it may conveniently be broken down into two parts. The first is the broad high contained within the 10γ contour, with an associated belt of lows roughly outlined by the zero contour, which runs from the southeast, across the top of the pyramid and off to the northwest. Superimposed on this general high-low pattern is a further region of high values confined within the 26γ contour. The very high gradient along the northern and eastern margin of the broad high suggests an origin near surface while the extent and slope to the west

and south suggest that the high is caused by a relatively large body at greater depth.

To effect a quantitative interpretation of this anomaly, we have designed a program to compute the anomaly due to any three-dimensional rectangular block as measured on the surface of an approximately equivalent cone. This program could equally well compute the anomaly on the actual surface, but this would require digitization of the topographic map, a step considered unnecessary for the present interpretation. The method of computation is that outlined by Bhattacharyya (1964).

An important assumption involved in all the discussion to follow is that the anomalies observed are the result of induced magnetization and that remanent magnetization is negligible. The separation of the two effects is a major problem when dealing with high iron minerals such as are anticipated here in the basalt. Probably the only satisfying comment that can be made about this situation is that if the remanent magnetization is strong, i.e. as strong as the induced, there will still result a strong anomaly that will certainly be interpreted as a magnetic body, but the interpreted body may be in error. Only rarely will the magnetic bodies be placed in such a fashion that the two fields cancel. That remanence is a problem in this survey is undoubted, since the only known piece of basalt detected (the small isolated 6 low mentioned earlier) had a remanent inverted anomaly.

In large structures, platforms, walls, etc., the remanent field of each piece of basalt used in the construction will cancel leaving the induced anomaly. It will be safe to proceed with the induced-only interpretation if the anomaly is large and "complicated" in this sense. The interpretational blocks are thus assumed to have no remanence.

The use of such blocks represents the practical limit of complexity in interpretational models. Since, by its very nature, the potential field is non-unique, there is nothing to be gained using models with greater shape variability. As with all indirect techniques, it is necessary to choose a model which is geologically realistic and which provides a good general fit to the data. This process, while not presenting a "true" picture of the causative body does allow estimation of the extent of the body and its depth limits. Presumably in archaeological studies even more restraints may be placed on the model to improve reliability. In the present case, for example, it is expected that any significant structures will be basalt so that a susceptibility value may be assigned to the model. Further, sharp discontinuities are expected between any structure and the surrounding clay or sand, whereas in the normal mineral exploration survey the magnetic rock unit may have a very poorly defined or irregular contact causing the anomaly to spread misleadingly.

In this interpretation a value of $10^{-3}$ e.m.u. has been assigned for the susceptibility of the model material in order to represent an average basalt. In their study of the rock types used in Olmec monuments, Williams and Heizer (1965) describe most of the rocks used at the La Venta site as olivine basalt with scattered magnetic grains which would certainly not

classify them as iron deficient. Assuming a normal basalt, and since roughly 50 percent of the basalts tested by Slichter (1942) had susceptibilities between $10^{-3}$ and $4 \times 10^{-3}$ e.m.u., it is evident that the choice of $10^{-3}$ is in fact conservative.

The values have been calculated for points on the surface of an equivalent cone; these project in plan to an equidimensional grid. These points are then contoured within the computer program and the resulting anomaly is plotted by a CALCOMP plotter. The computer drawn maps for the detail map area are on the same scale as the data plot, Figure 5. All data has been plotted with the vertical margin of the plot corresponding to magnetic north. For all the calculations in this study, the Earth's field is assumed to be 44,000$\gamma$ with an inclination of 45° and a declination of 8°30' west of geographic north. The equivalent cone is 30 m high and 80 m in radius.

The horizontal location of a block will be given in a plan drawing, with the vertical coordinate (Z) and the half height ($\Delta z$) written on the drawing. The x coordinate is positive north, y positive east, and z positive <u>up</u>, all with respect to the base and center of the pyramid.

From a preliminary inspection of the anomaly, it may be suspected that the anomaly could be the result of a discontinuity in the susceptibility of the surface soil layer. Since the block models have sides that parallel the coordinate axis, models representing layers parallel to the pyramid slope must be approximated by horizontal slabs with an appropriately corrected inclination. A second program was written to calculate the field observed on a horizontal grid above a horizontal slab thus approximating the pyramid surface over a limited area by a flat plane. These anomalies were calculated and plotted for the detail area as in the block model and are also presented in the same scale as the detail map, Figure 5.

Values of soil susceptibility are usually less than $10^{-4}$ e.m.u. and certainly the susceptibility contrast will be even less for natural soil gradations. Further, natural soils will not possess abrupt discontinuities so maximum effects may be calculated using thin slab models with vertical boundaries.

A large slab 10.5 meters on a side and of varying thickness has been chosen as a representative model for the anomaly in Figure 5. The resulting contour maps for slab thicknesses (h) of 0.5, 1.0, 2.0, and 4.0 meters are shown in Figures 8 to 11. The outline of the slab is shown in heavy dotted lines in Figure 8. To assist in the study of these models and their relationship to the field data, the N-S profiles, B-B', through each contour map are presented in Figure 22 and these may be compared to profile B-B' of Figure 5.

In all models the anomalies were obtained for a sensor height above the slab of 0.5 meters.

It is obvious from these plots that a thin discontinuous soil layer (0.5m) cannot produce the observed anomaly either in character or in

amplitude. The extremes of the anomaly occur close to the nothern and southern margins of the body and the maximum value is less than 6γ. Increasing the susceptibility from $10^{-4}$ to $5 \times 10^{-4}$ would amplify the anomaly magnitudes appropriately but would preserve the isolation of the high and the low.

As the thickness of this slab increases, however, the anomaly, at least in the profile shown, becomes remarkably similar to the observed data. The slab 4 meters thick has roughly the same "width" (indicated by $\Delta_{x_1}$ on the profile, Figure 22) on the south as the field data, but is not nearly as wide ($\Delta_{x_2}$) on the north as the field data. While this thick slab represents the central N-S profile quite well it fails in other respects. The field data is quite asymmetric in an East-West profile as section A-A' of Figure 19 shows, and the low area bounding the eastern and northern edges of the anomaly, trends off to the north west rather than wrapping around on the west as the slab model does. The model could probably be converted to a wedge, thickening to the East but this shape would be too costly to model with the existing techniques.

The result of this interpretation using the slab model is that the anomaly could be produced by some slab-like body at least 4 meters thick with a susceptibility of $10^{-4}$ approximately. Possibilities are: (1) a pit filled with highly organic soil, (2) a pit filled with stone other than basalt. It is difficult to imagine a pit of this composition and dimension showing no erosional expression or no surface gological expression. In fact, comparing the magnetic data (Figure 5) and the topographic map for the same area (Figure 7), it can be seen that there is no apparent correlation between the proposed pit and the topography. Should the pit have been filled with a less susceptible stone than basalt (e.g. serpentine) then a significant archaeological structure is still indicated.

The above interpretation is restricted by the susceptibility assumed for the slab material. To expand the interpretation to include the typical basalts that have been assumed for monument material requires the model structures to be at greater depth. For example, if the preceding slab models were of basalt the anomalies would be increased tenfold. The 0.5 widths, $\Delta_{x_1}$ and $\Delta_{x_2}$, would be too small to approximate the field profile. (Increasing the susceptibility simply multiplies the anomaly but does not change the position of the peaks, troughs, zero crossings, etc. in the horizontal dimension). To increase these model widths it would be necessary either to deepen the slab or increase its thickness, and the latter process would of course make the amplitude of the anomaly too high. After a number of such models (i.e. slabs of basalt at varying depths) were processed, it was found that deepening the model destroyed the essential character of the field profile and worsened the fit around the margins.

Turning to the "standard" buried block models now becomes a matter of trial and error fitting procedures. This process is extremely tedious and

also quite costly in computer time so that in the present analysis it has not been continued beyond a model that provides a basic fit. From this basic fit and from a knowledge of the behaviour of the anomalies from bodies of varying parameters, it is possible to postulate a number of likely configurations for the actual causative body.

Single block models proved early in the interpretation to be inadequate. This combination of the steep gradients around the margin and broad high to the south necessitated multiple bodies. Wall-like structures were then placed close to the surface to provide the steep gradients and the final configuration achieved is shown in the plan diagram, Figure 12, as Model 5.

These plan diagrams have the elevation of the top of each block written on the block. The surface elevation of the pyramid at a point directly above that corner of the block which comes closest to the surface is noted in the plan view just off the block. It is assumed that the sensor is positioned on the equivalent surface. Thus in speaking of depth of a body below the surface the depth is actually that below the sensor.

The east-west wall of Model 5 is higher than the north-south wall, but the north-south wall comes within 1.0 meters of the surface, accounting for the 18γ peak to the south in Figure 15. The A-A' and C-C' profiles of Figures 19 and 21 show a fairly good fit in general shape for the two walls alone, but it is evident that the whole anomaly must be "pushed up" and that the north wall should be brought closer to the surface.

To effect the general uplift and broadening of the model anomaly large blocks of basalt at depth were added to the model. Model 5b is a combination of the two walls mentioned previously and a large block (4 x 4 x 6 meters, off center, and with its center 10 m above the base as shown in Figure 12). The A-A' and C-C' profiles for Model 5b show the result of this combination. The amplitude is in fact raised but the plan view of the anomaly shows the inadequacy of the result. No single large block (which would play the role of a major structure, such as a stone sub-pyramid within the pyramid) could be found to raise the central area of the anomaly (say the area within the 16γ contour of Figure 5). This area appears to be a magnetic platform upon which are superimposed wall-like anomalies. A wide flat slab, subparallel to the pyramid surface could result in this effect.

There is also the problem of the 30+γ high just off the N-S center line, below center, in Figure 5. This might be the effect of another block, but a single block here would have a marked low to the north rather than the gentle dip seen in Profile B-B', Figure 20.

The 30+γ high and the general area of values greater than 20γ were finally well approximated with the wall-plus-horizontal slab model (Model 6a) of Figures 13 and 16. In this model a thin (0.5m) horizontal slab forms a base for the two walls. The slab itself comes within 1.0 meter of the surface, the east-west wall within 1.0 meter, and the north-south wall within 1.5 meters. The resulting fit as seen in the contour maps is

good, except for the fact that, again, the whole model anomaly needs to be pushed up and that the west side of the anomaly has to be stretched out considerably. Profile B-B' of Model 6a has a slightly smaller width on the north than the field data, indicating that the actual body is slightly deeper than the model. Profiles C-C' and A-A' of the field data are both taken over sections of maximum gradient, and the model profiles for 6a have approximately the same widths. These results indicate that the body is within 0.5 meter of the surface. It is more realistic however to consider the contour map itself and realize that the average width of the anomaly along the northern and eastern margins is greater than in the cross sections illustrated. The extreme low to the north is, as mentioned previously, almost certainly the result of another body farther north and the low (less than -10$\gamma$) on the east is due to accentuation by topography. This topographic effect is brought about by the gully coinciding with the low area thus bringing the sensor closer to the body in this area and increasing the magnitude of the anomaly. The position of the minimum in profile A-A' is thus shifted inward giving a false indication of depth.

This same topographic effect is responsible for the 30+$\gamma$ peak's being isolated in the field data and an elongate ridge in the model. The high occurs in a gully where the observations were closer to the slab and thus higher in amplitude.

Model 6b is a variation of Model 6a wherein the platform has been dropped 0.5 m, the east wall brought within 0.5 m of the surface, and the north wall lowered 0.5 m. Model 6b provides a better fit to the field data in profile B-B' and to the east in profile A-A'.

To generalize these results, considering the topographic effects and the average width of the anomaly, it may be concluded that the walls assumed for the interpretation come within 1 - 2 meters of the surface of the pyramid.

None of the models presented accounts for the general magnetic high in the anomalous area nor for the gradual slope of the anomaly to the west. Nor do these models account for the fact that the magnetic low with the associated steep gradient runs off to the northwest instead of wrapping around to the southwest. This latter anomaly could be explained by placing another wall, starting at the western edge of the existing wall (block 3 of Figure 13) and running approximately NW for 10 to 15 meters.

In conclusion, the interpretation that emerges from these models may best be summarized in the following point form:

(a) The general magnetic high within the 16$\gamma$ contour of Figure 5, or alternately the yellow area and higher of Figure 6 may be explained by a substructure within the pyramid. The center of mass of this body is displaced due south of the pyramid center by as much as 30 meters. None of the simple models that were used in the interpretation were successful in representing this feature. A slab-like body, possibly parallel to the pyramid surface, at a depth of 3 - 6 meters could be one explanation. It will be noticed in comparing

the magnetic map (Figure 5) and the topographic map (Figure 7) that the two limbs of the magnetic high that develop to the south correspond almost exactly with two ridges that develop in about the center of the map area. The magnetization of the ridge and gully topography, high on the ridge and low in the gully is responsible for the split pendant shape of the general magnetic high. This effect is even more evident in the color shaded map.

(b) The detailed structure at the top is well represented by a thin slab platform with superimposed walls on the eastern and northern edges. "Walls" might well be basalt columns and the platform a pavement surface of small blocks. In order that the reader not be carried away with this interpretation, we add that the anomaly could also be caused by a rubble level of basalt blocks that simply come closer to the surface along the northern and eastern margin.

The major fact that emerges from the model interpretation is that the source of these anomalies near the top of the pyramid is almost certainly basalt and that it comes within 1 - 2 meters of the surface.

The precise location of the buried structure could possibly be outlined by probing the ground with steel rods. Alternatively the anomalies could be drilled at relatively low cost with a gasoline-powered auger or corer. These probings should be carried out in the vicinity of the magnetic highs. To dig the pyramid, the best technique would probably be to dig a trench running south from a point 4 meters east and 5 meters south of the center to a point 4 meters east and 13 meters south. From the southern end of this trench another trench should be run east into the gully for approximately 6 meters. These trenches should be at least 3 meters deep.

# FIGURES

# PLATES

Plate 1 Total packaged equipment for the magnetometer survey

a) Portable 350 watt generator (40 lbs.)

b) Case containing counter, couplers, fixed sensor, power supply, and power cable (50 lbs.)

c) Roving sensor (7 lbs.)

d) Coaxial cable reel for connecting fixed and roving sensors to the power supply and counter (25 lbs.)

Plate 2 Roving sensor and fixed sensor in operation

Plate 3 The read out unit

Plate 4 The read out unit

Plate 5 Clearing the underbrush from the pyramid

Plate 6 Roving sensor operator steadied by rope

Plate 7 Roving sensor positioned at 3 m mark on white cord

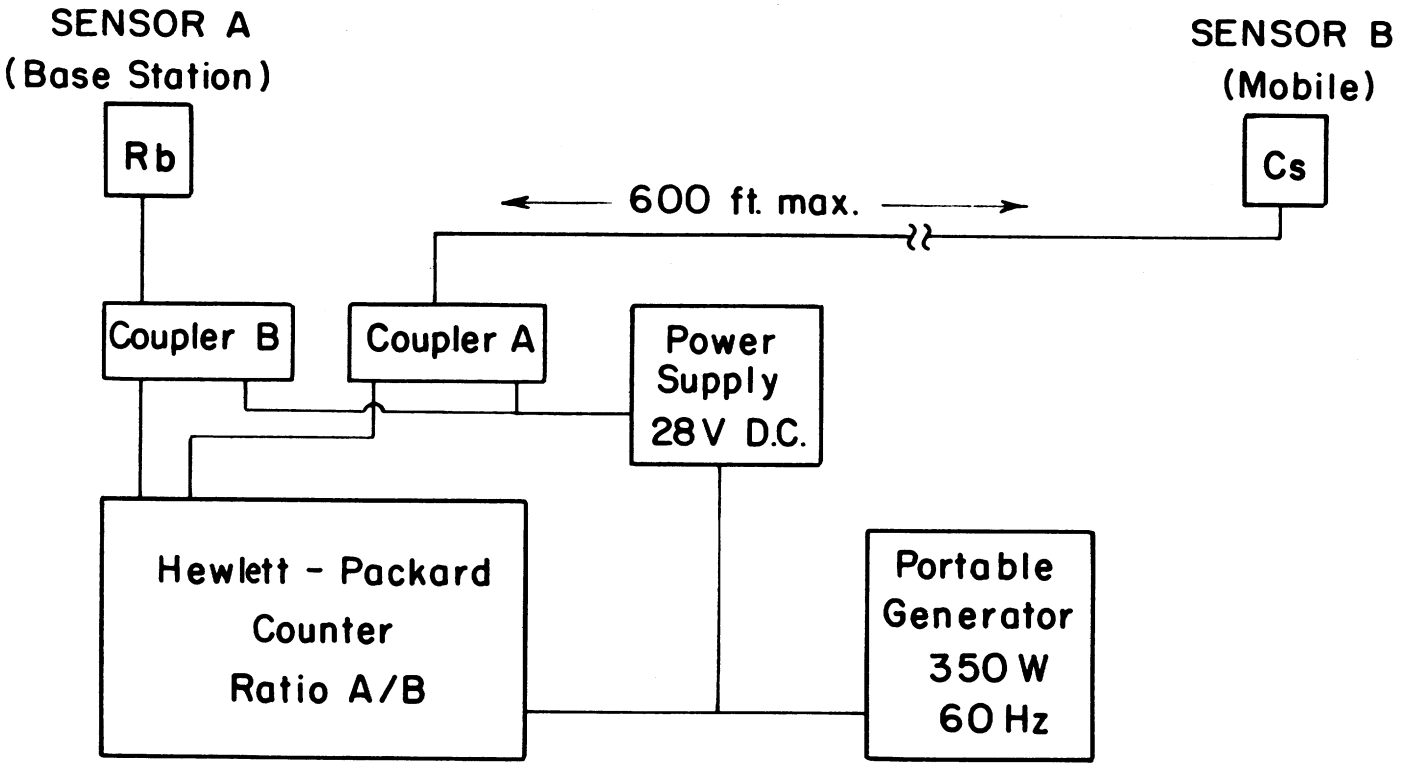


SCHEMATIC DIAGRAM OF MAGNETOMETER.

Figure 1

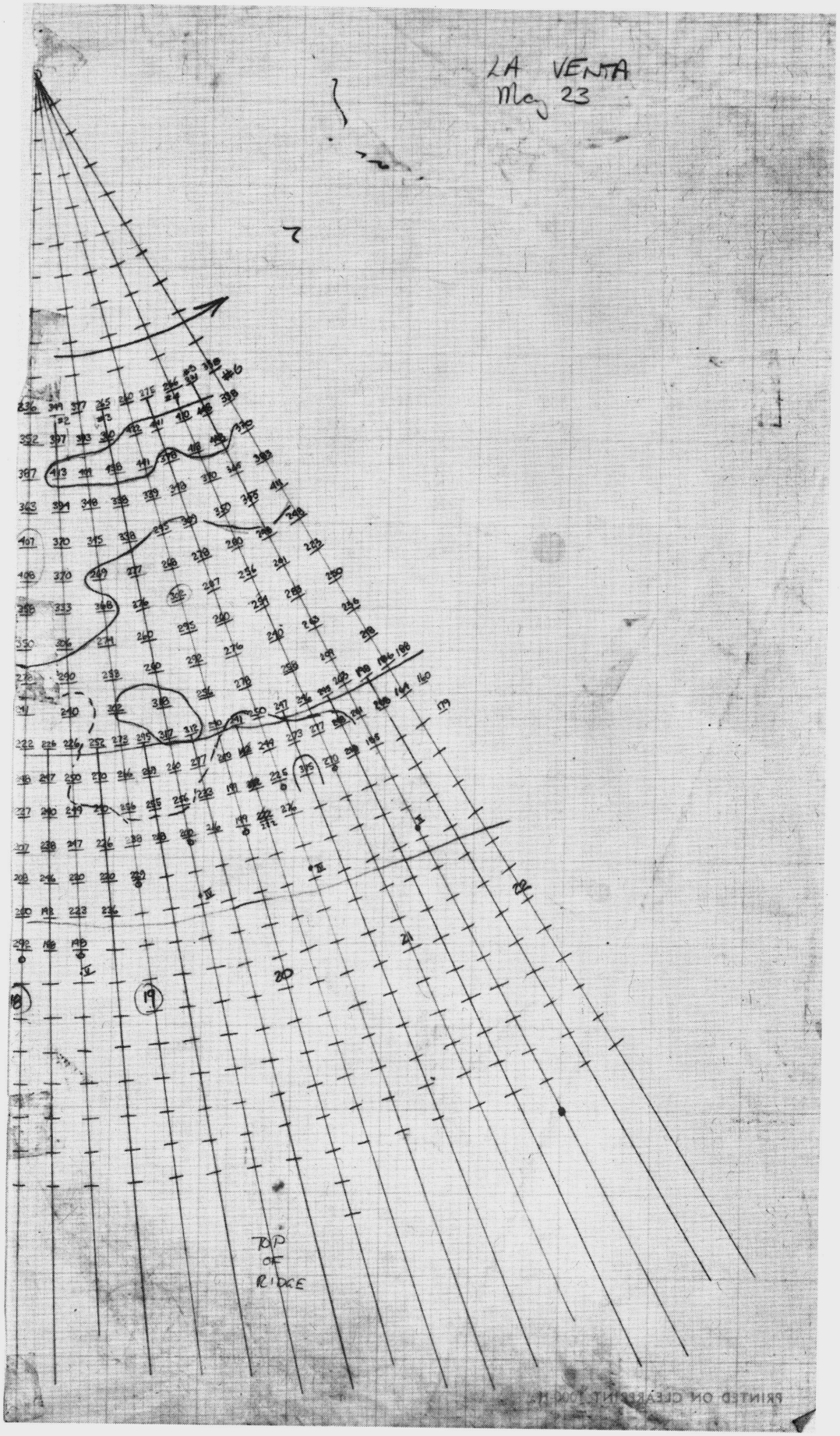


Figure 2

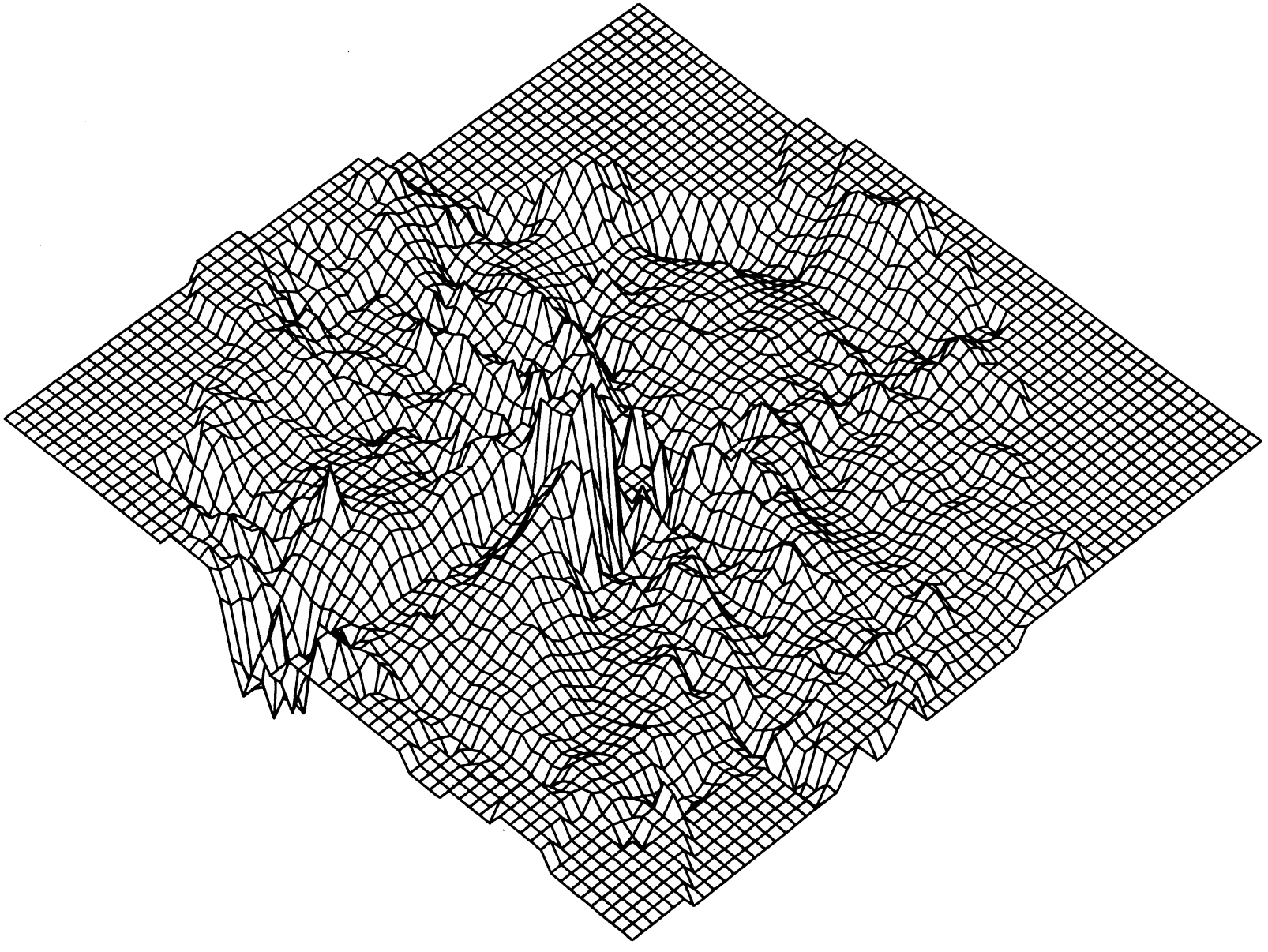

**PERSPECTIVE VIEW OF MAGNETIC MAP.**

Figure 3a

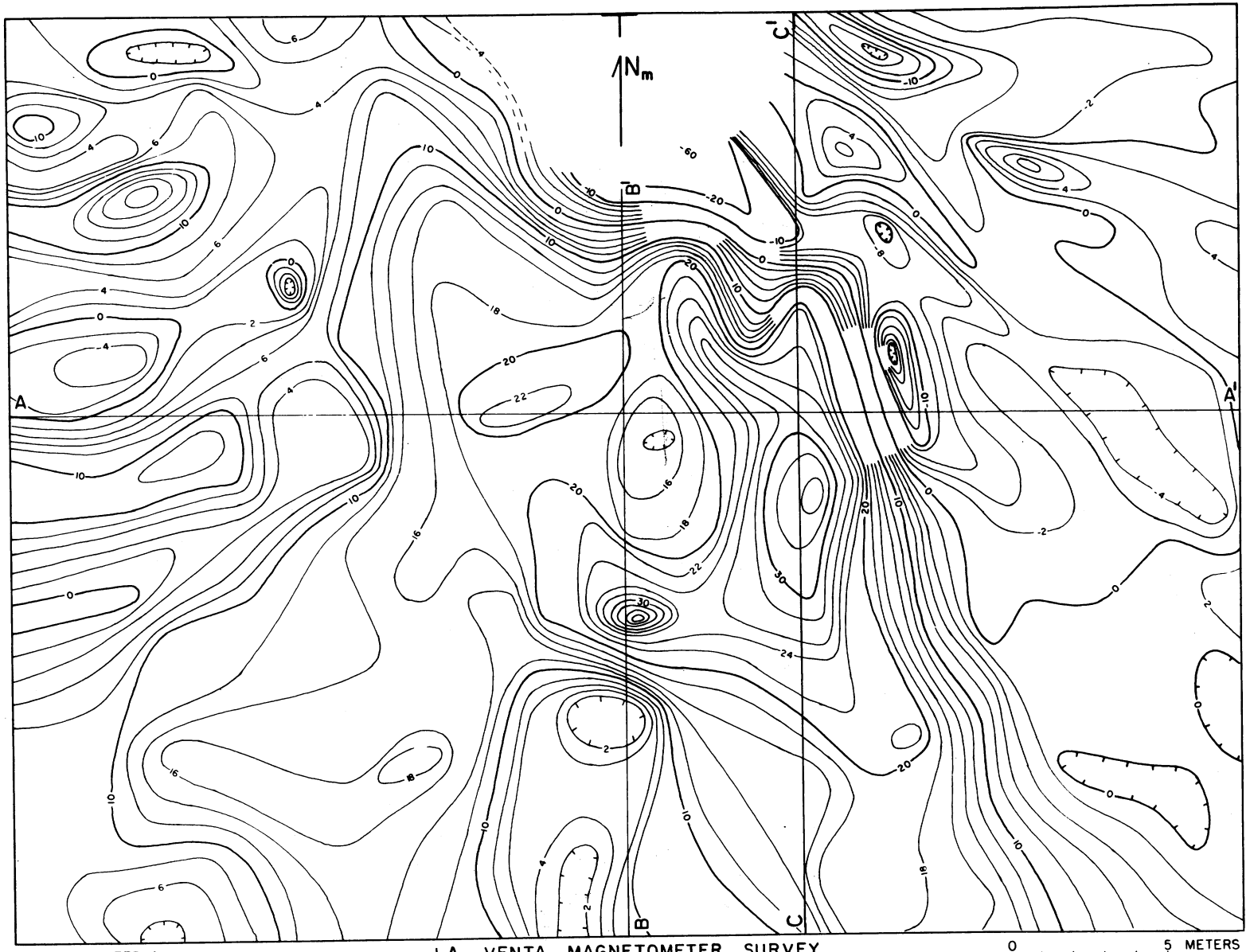
$N_m$
A
A'
B
B'
C
C'
CONTOUR INTERVAL:
2 GAMMAS
LA VENTA MAGNETOMETER SURVEY
DETAIL MAP
0
5 METERS

Figure 5

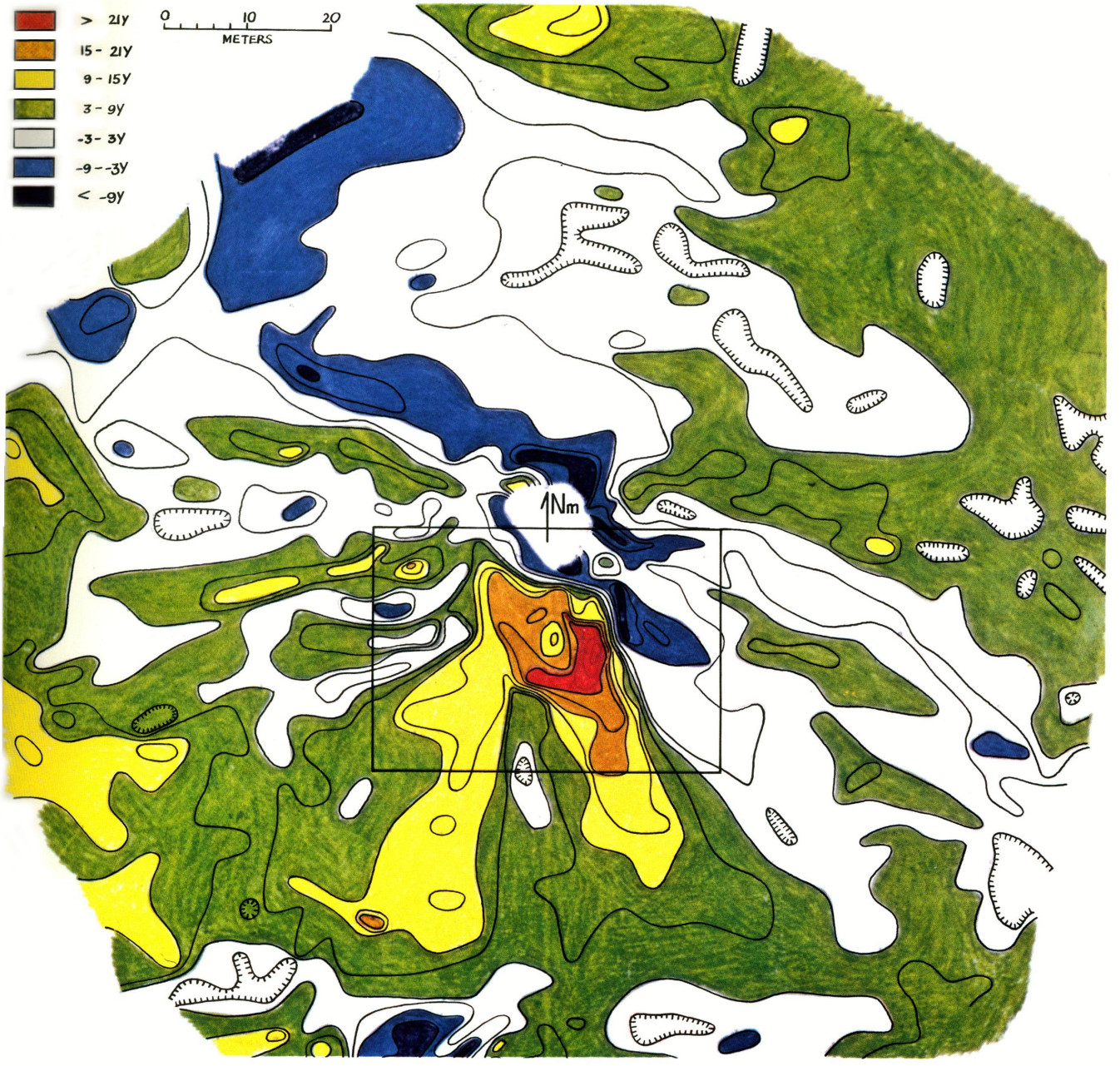


La Venta Pyramid
Magnetometer Survey

Figure 6

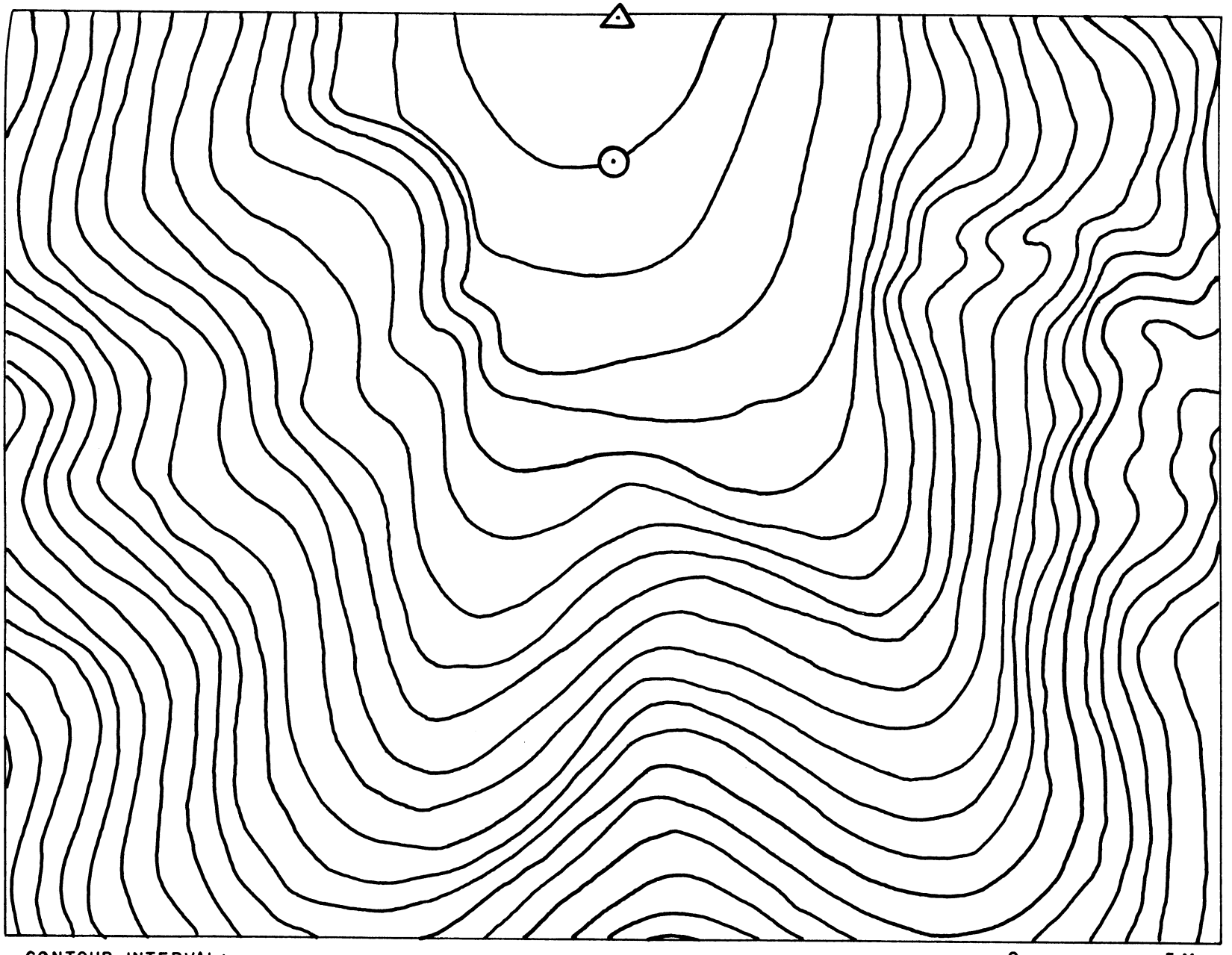
CONTOUR INTERVAL:
2 FEET
DETAIL MAP TOPOGRAPHY
FROM FIGURE 4
0
5 M

Figure 7

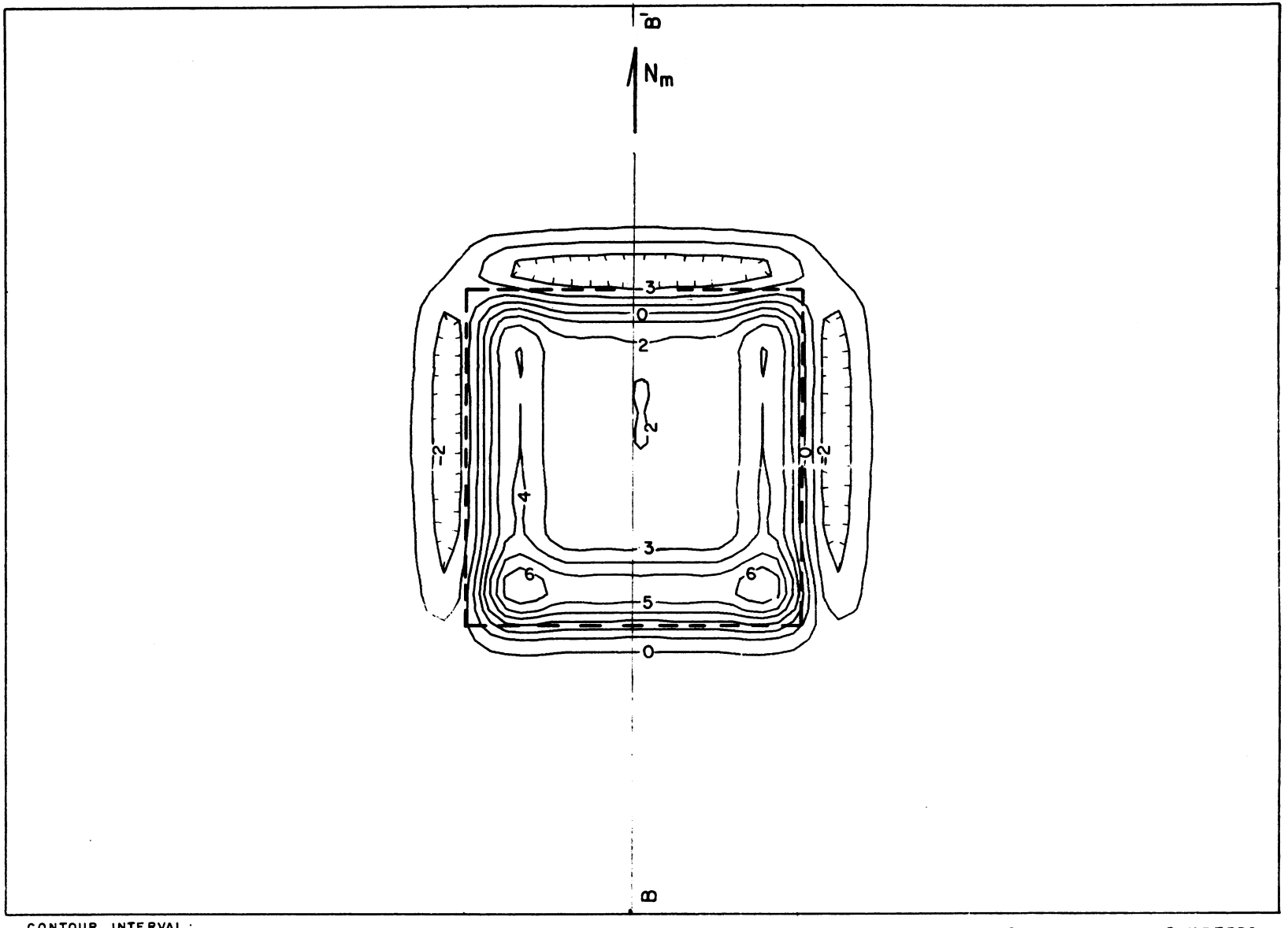


CONTOUR INTERVAL:
2 GAMMAS

0 5 METERS

MODEL 1

Figure 8

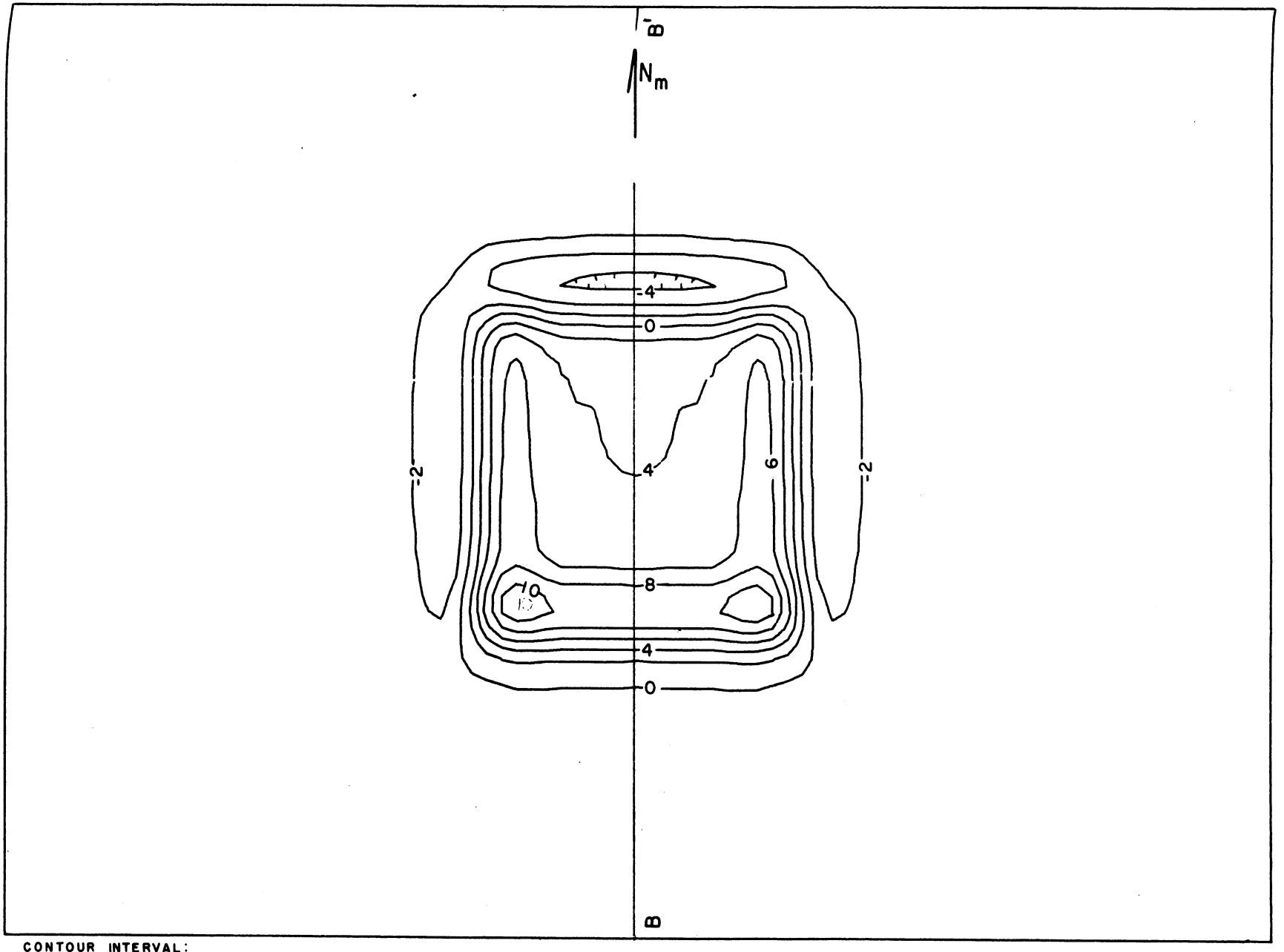
B
$N_m$
-4
0
4
8
4
0
-2
6
-2
10
B
CONTOUR INTERVAL:
2 GAMMAS
MODEL 2
0
5 METERS

Figure 9

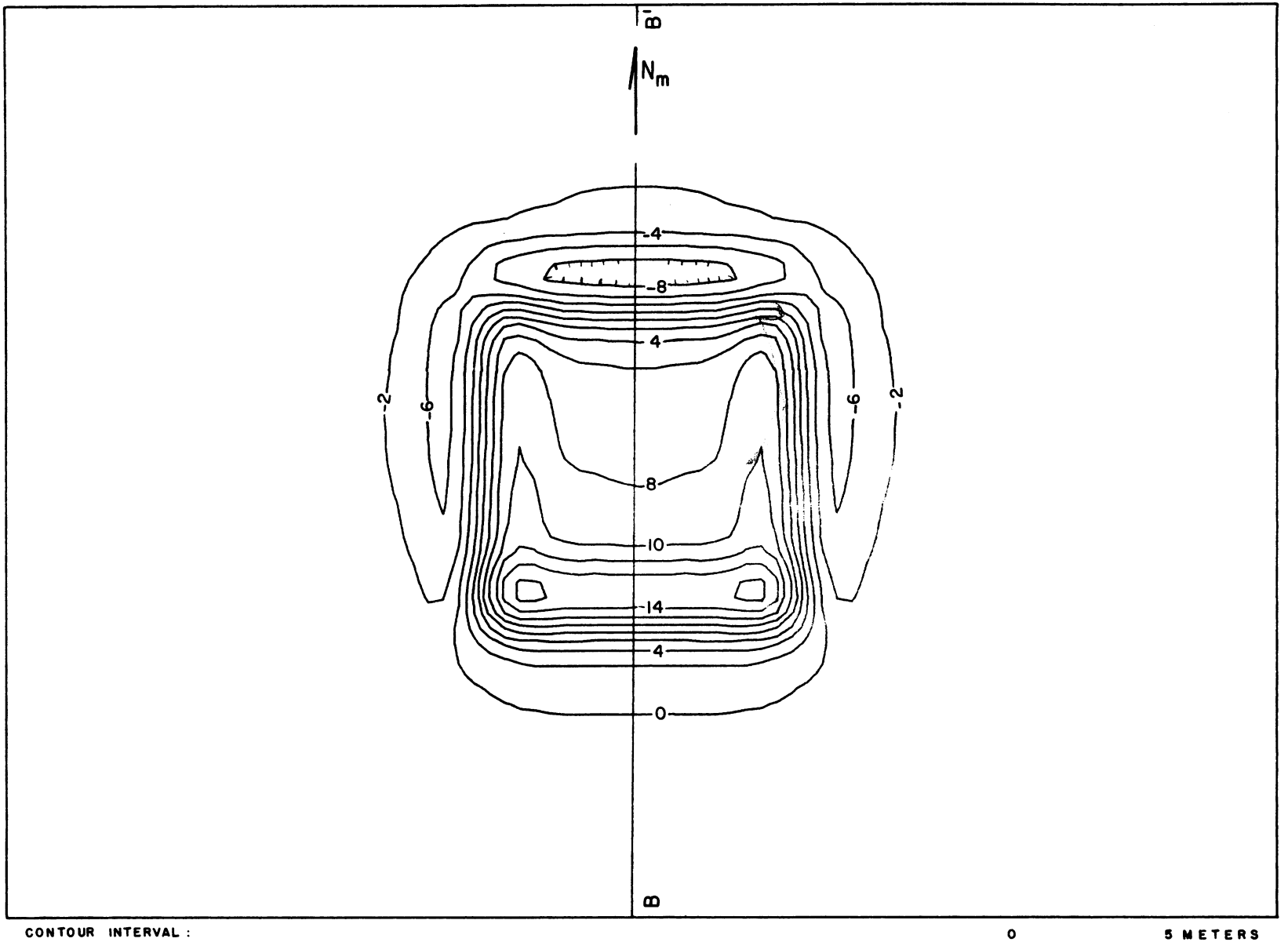
B'
$N_m$
-4
-8
4
-2
-6
-6
-2
8
10
14
4
0
B
CONTOUR INTERVAL :
2 GAMMAS
MODEL 3
0
5 METERS

Figure 10

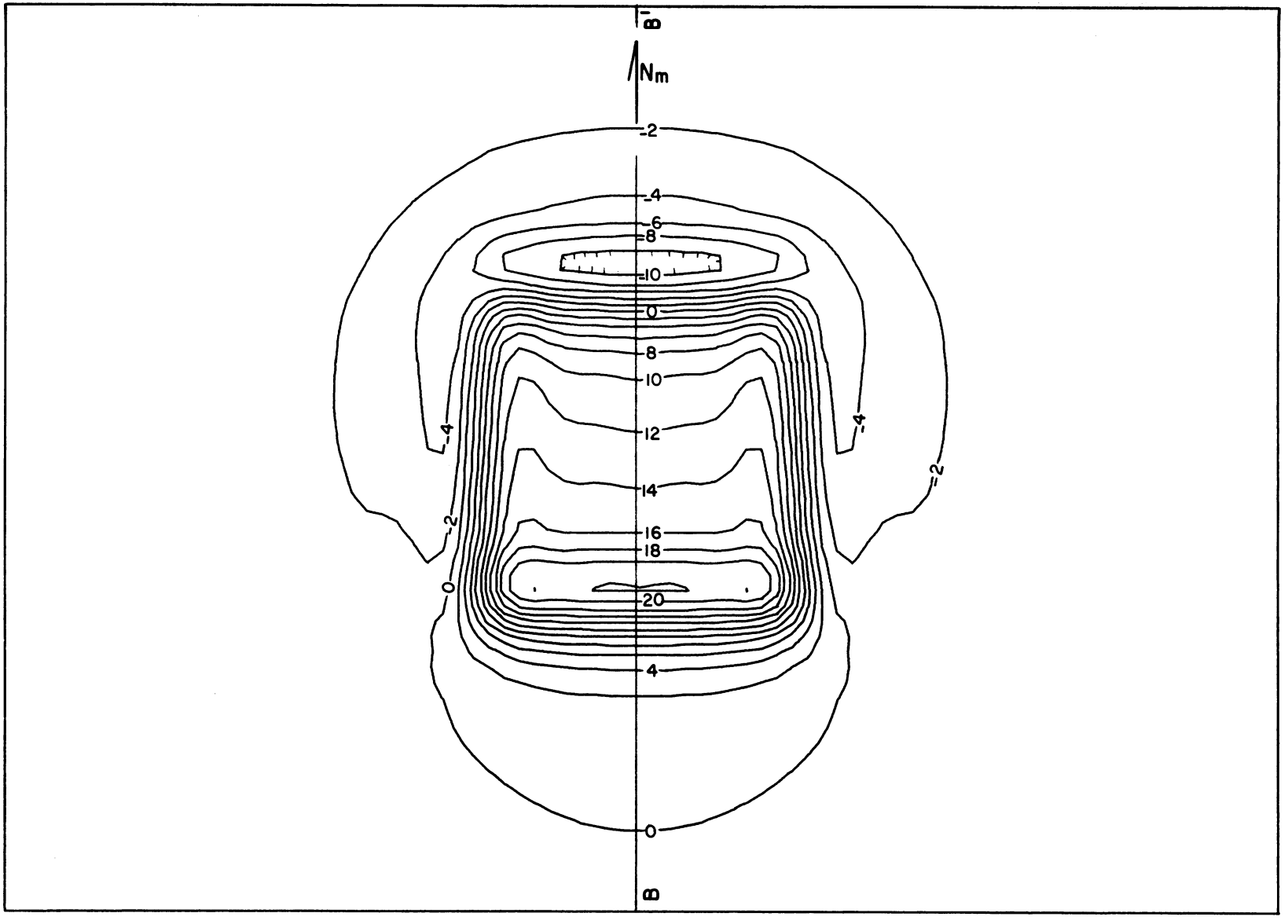


CONTOUR INTERVAL :
2 GAMMAS

MODEL 4

0 5 METERS

Figure 11

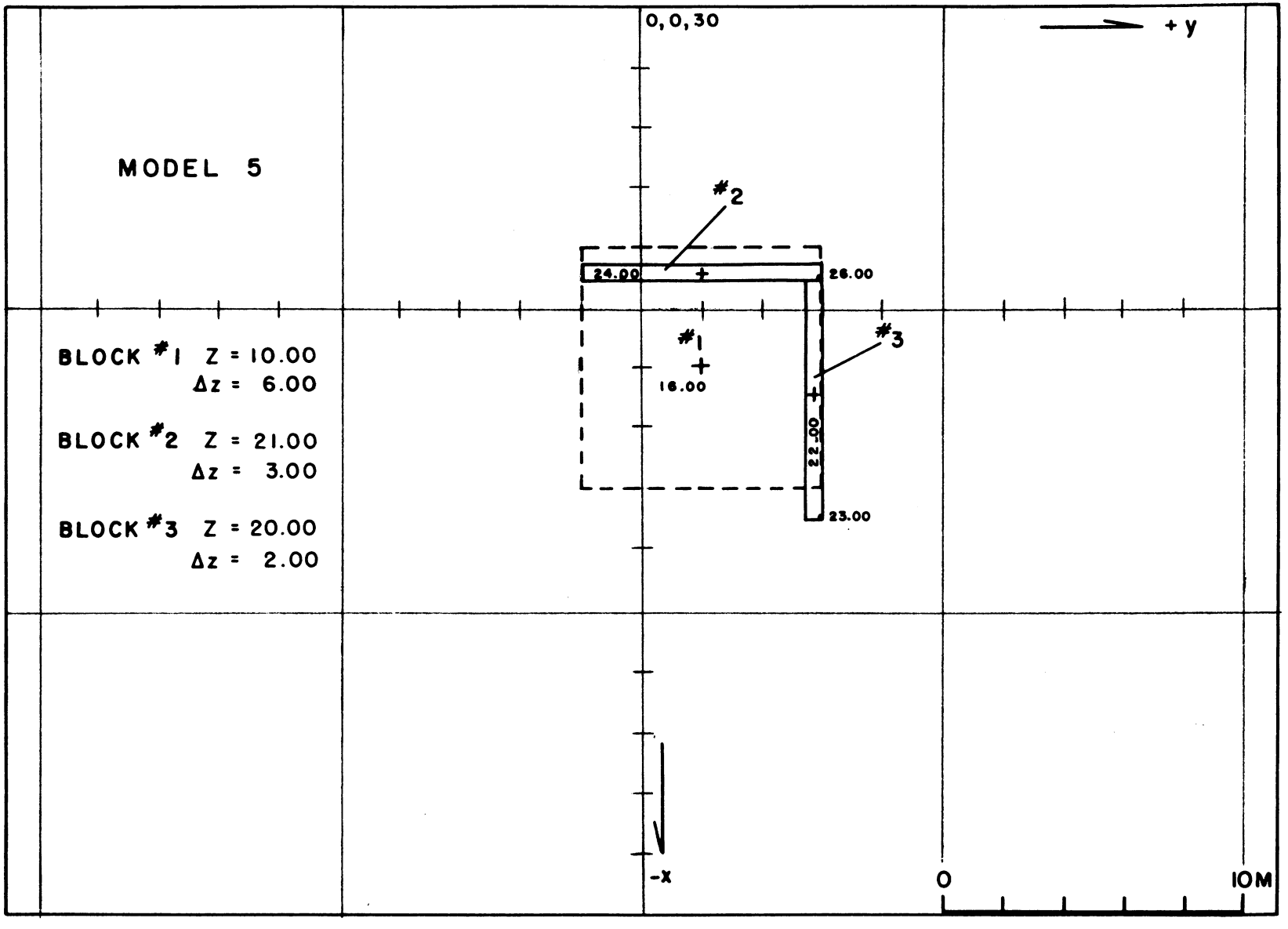
MODEL 5
BLOCK #1 Z = 10.00
Δz = 6.00
BLOCK #2 Z = 21.00
Δz = 3.00
BLOCK #3 Z = 20.00
Δz = 2.00
0,0,30
+ y
#2
24.00
26.00
#1
16.00
#3
22.00
23.00
-x
0
10M

Figure 12

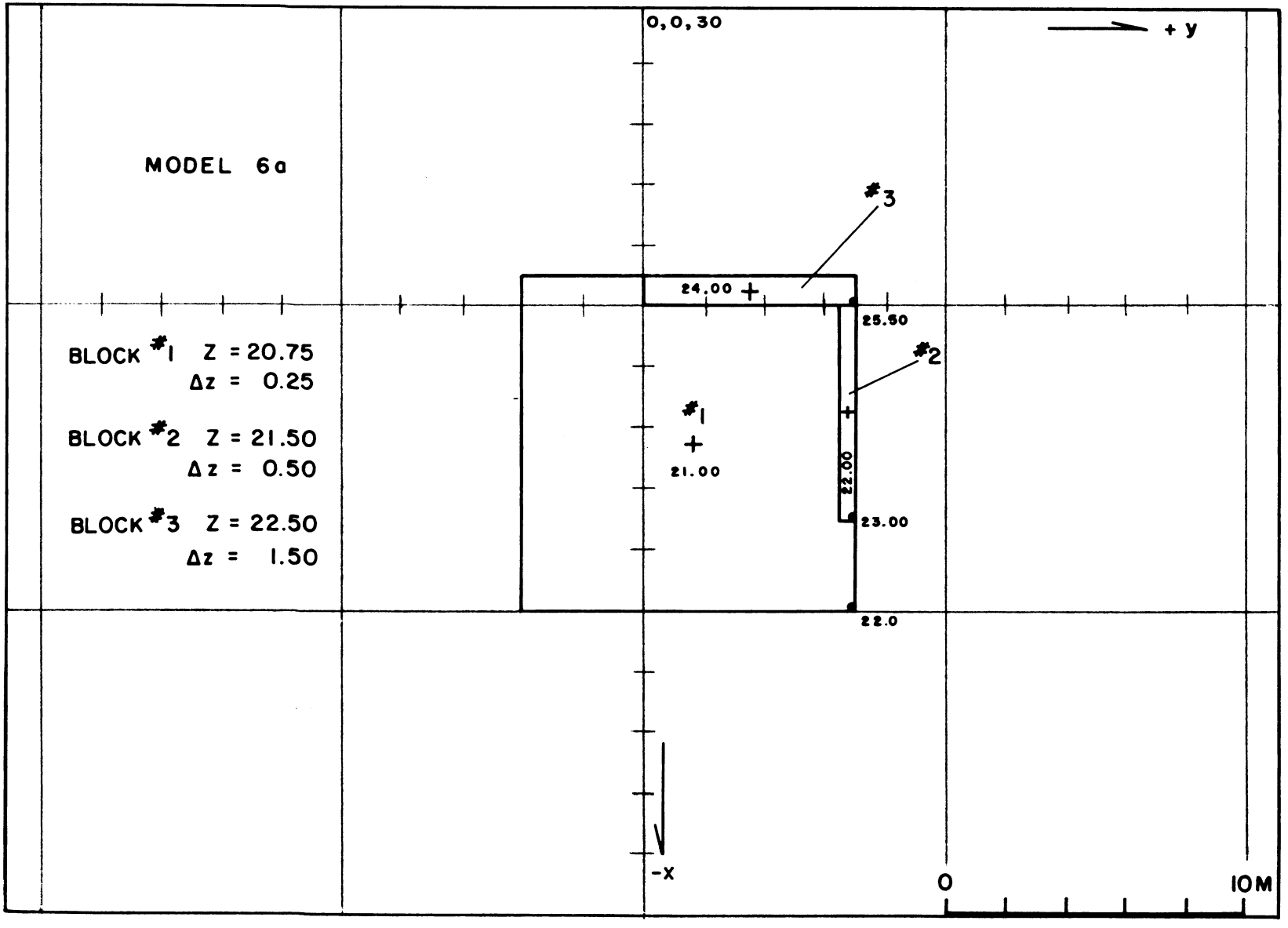
MODEL 6a
BLOCK #1 Z = 20.75
Δz = 0.25
BLOCK #2 Z = 21.50
Δz = 0.50
BLOCK #3 Z = 22.50
Δz = 1.50
0,0,30
+ y
#3
24.00
25.50
#2
#1
21.00
22.00
23.00
22.0
-x
0
10M

Figure 13

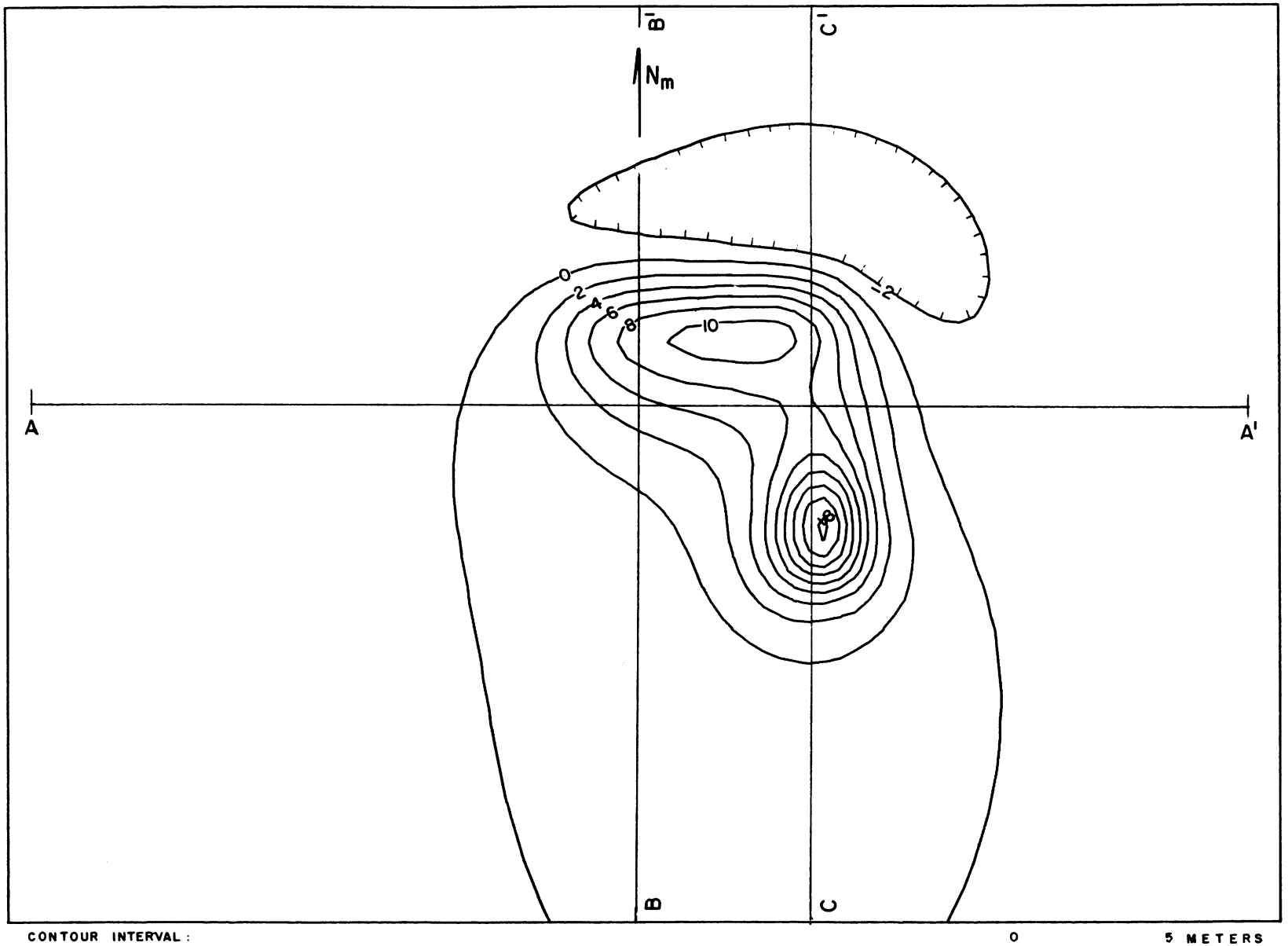
B'
C'
$N_m$
0
2
4
6
8
10
-2
A
A'
B
C
CONTOUR INTERVAL:
2 GAMMAS
MODEL 5a
0
5 METERS

Figure 14

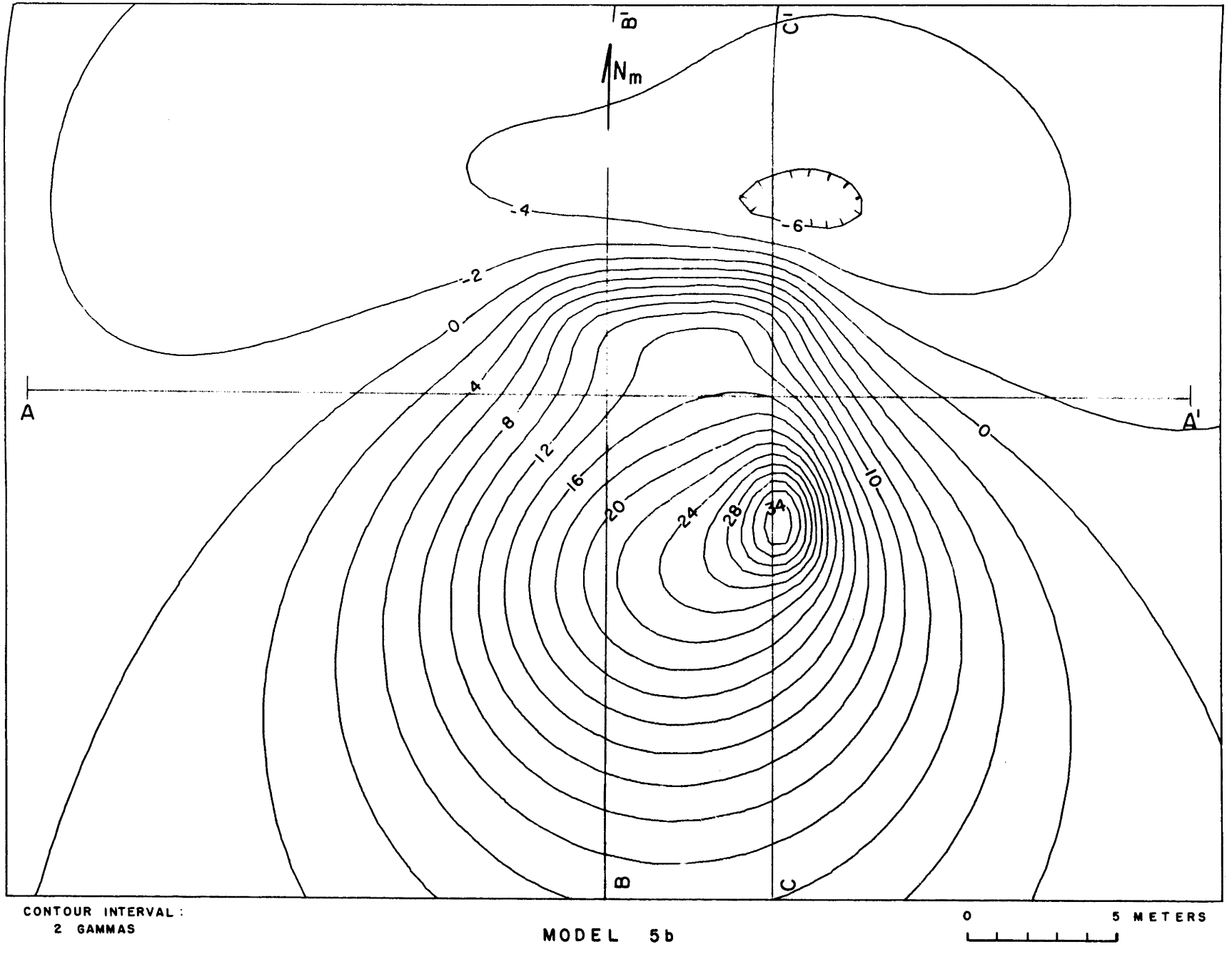
B̄
C̄
Nm
-4
-6
-2
0
4
8
12
16
20
24
28
34
10
0
A
A'
B
C
CONTOUR INTERVAL :
2 GAMMAS
MODEL 5b
0
5 METERS

Figure 15

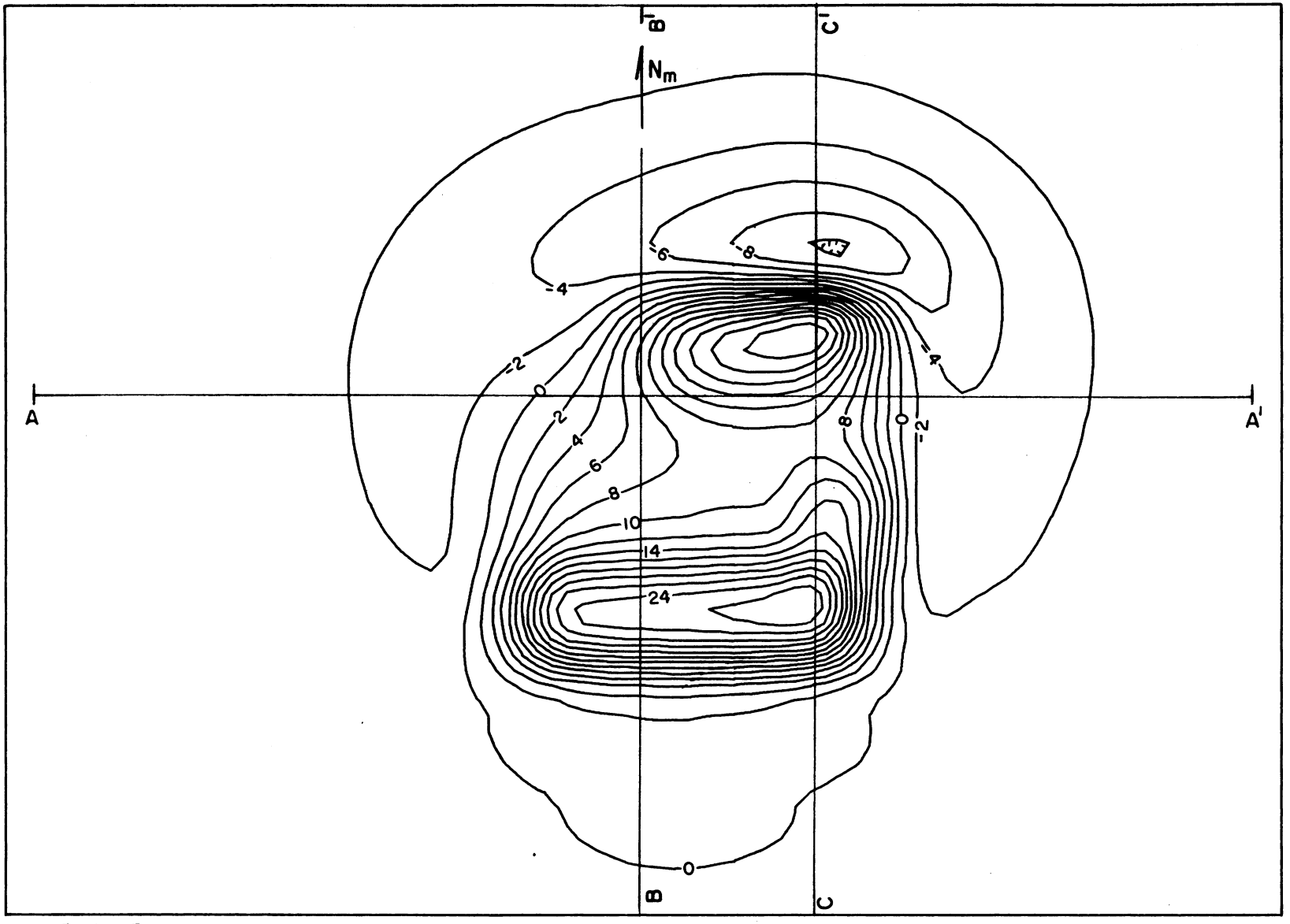
B'
C'
$N_m$
-6
-8
-4
-2
0
2
4
6
8
10
14
24
A
A'
B
C
CONTOUR INTERVAL:
2 GAMMAS
MODEL 6a
0
5 METERS

Figure 16

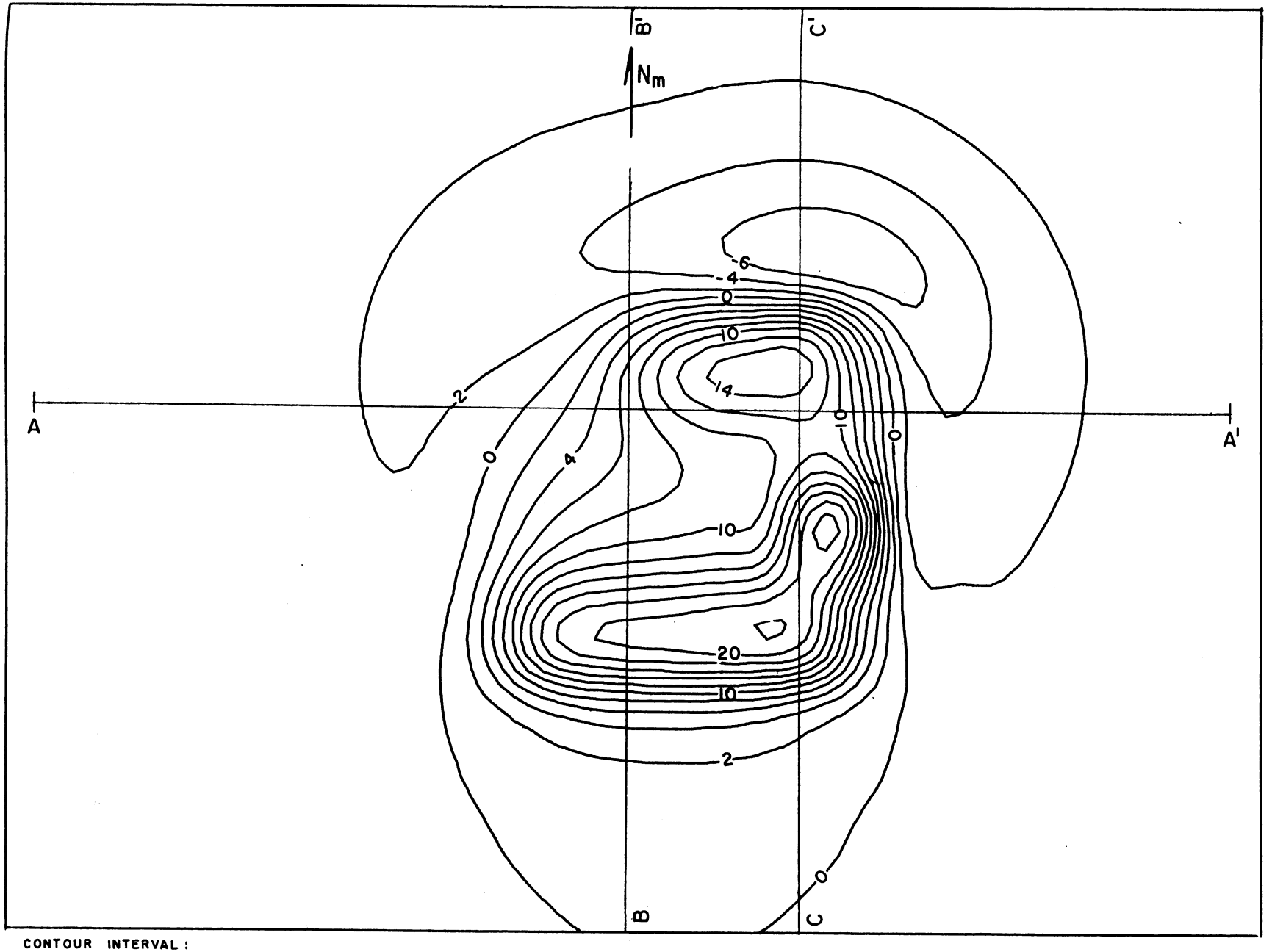


CONTOUR INTERVAL:
2 GAMMAS

MODEL 6b

0 5 METERS

Figure 17

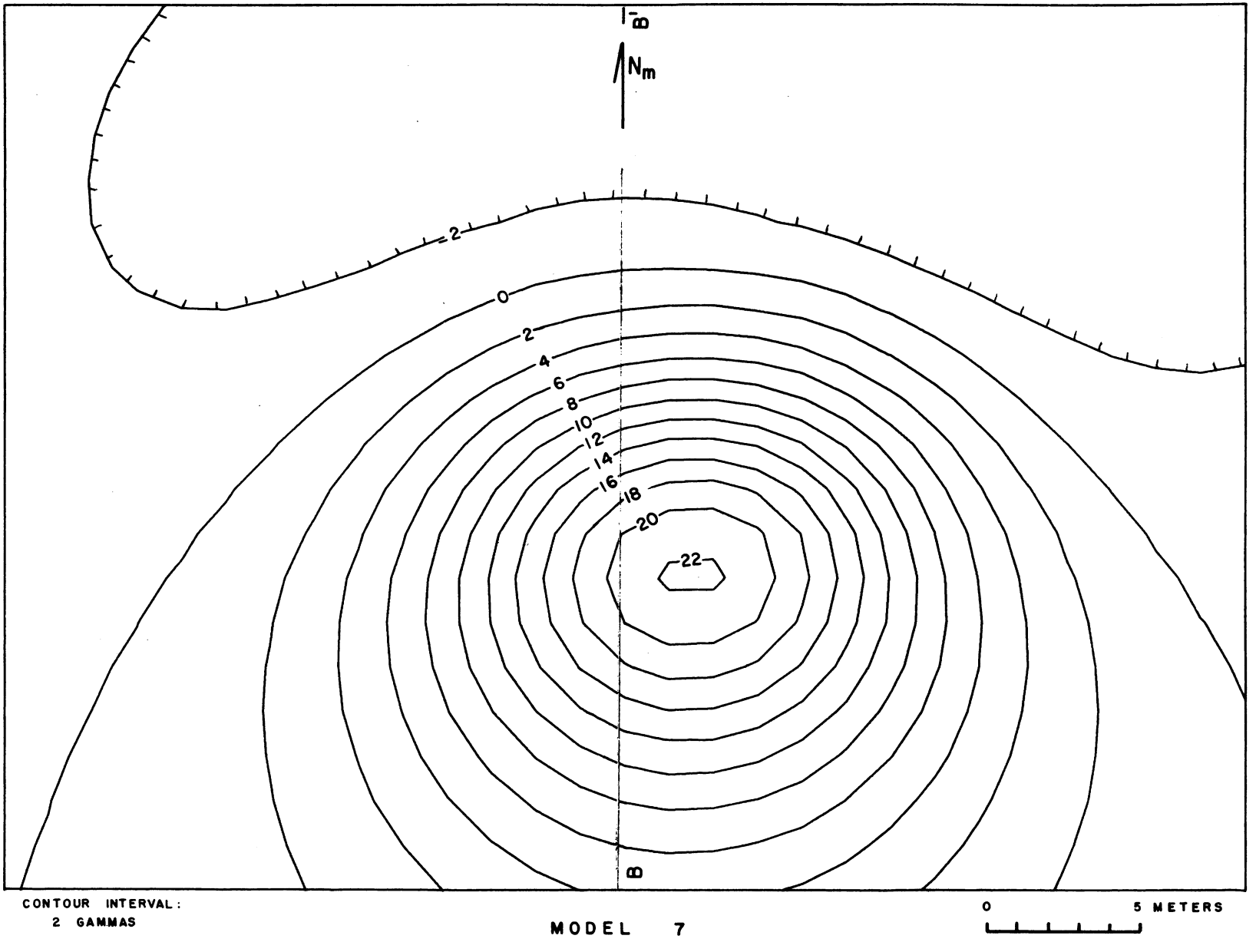
B
$N_m$
-2
0
2
4
6
8
10
12
14
16
18
20
22
B
CONTOUR INTERVAL:
2 GAMMAS
MODEL 7
0
5 METERS

Figure 18

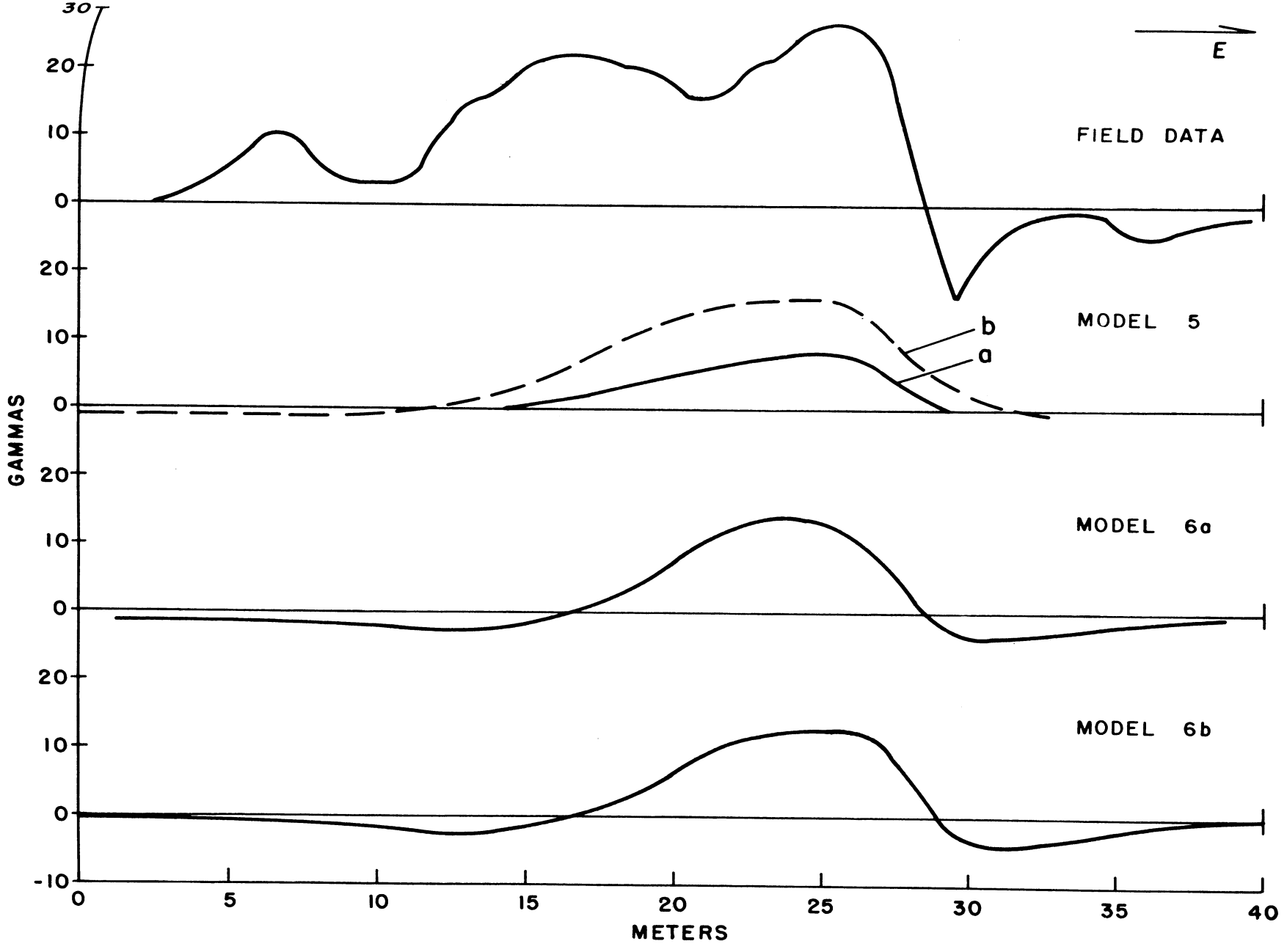


MAGNETIC PROFILES A-A'

Figure 19

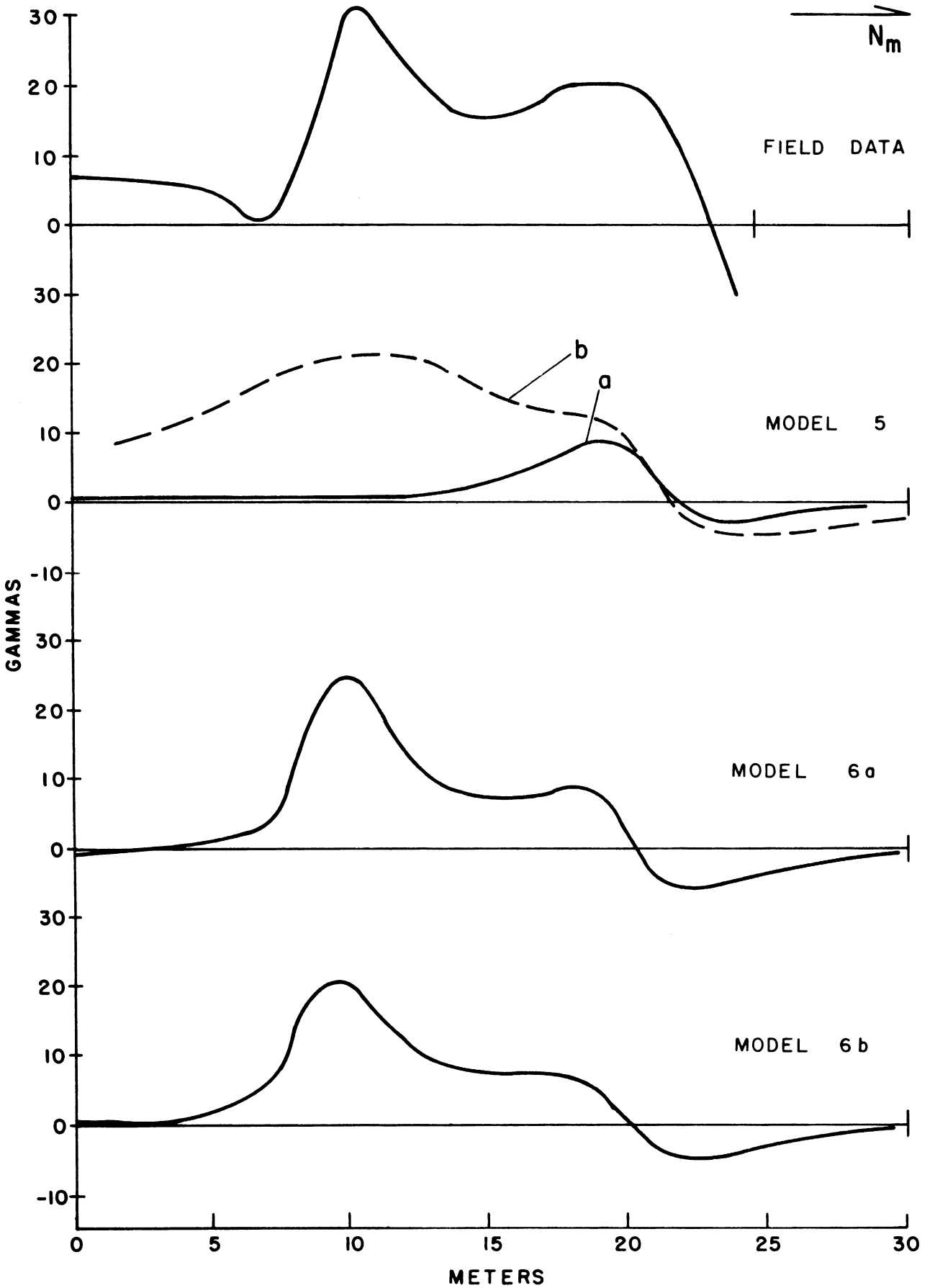


MAGNETIC PROFILES B-B'

Figure 20

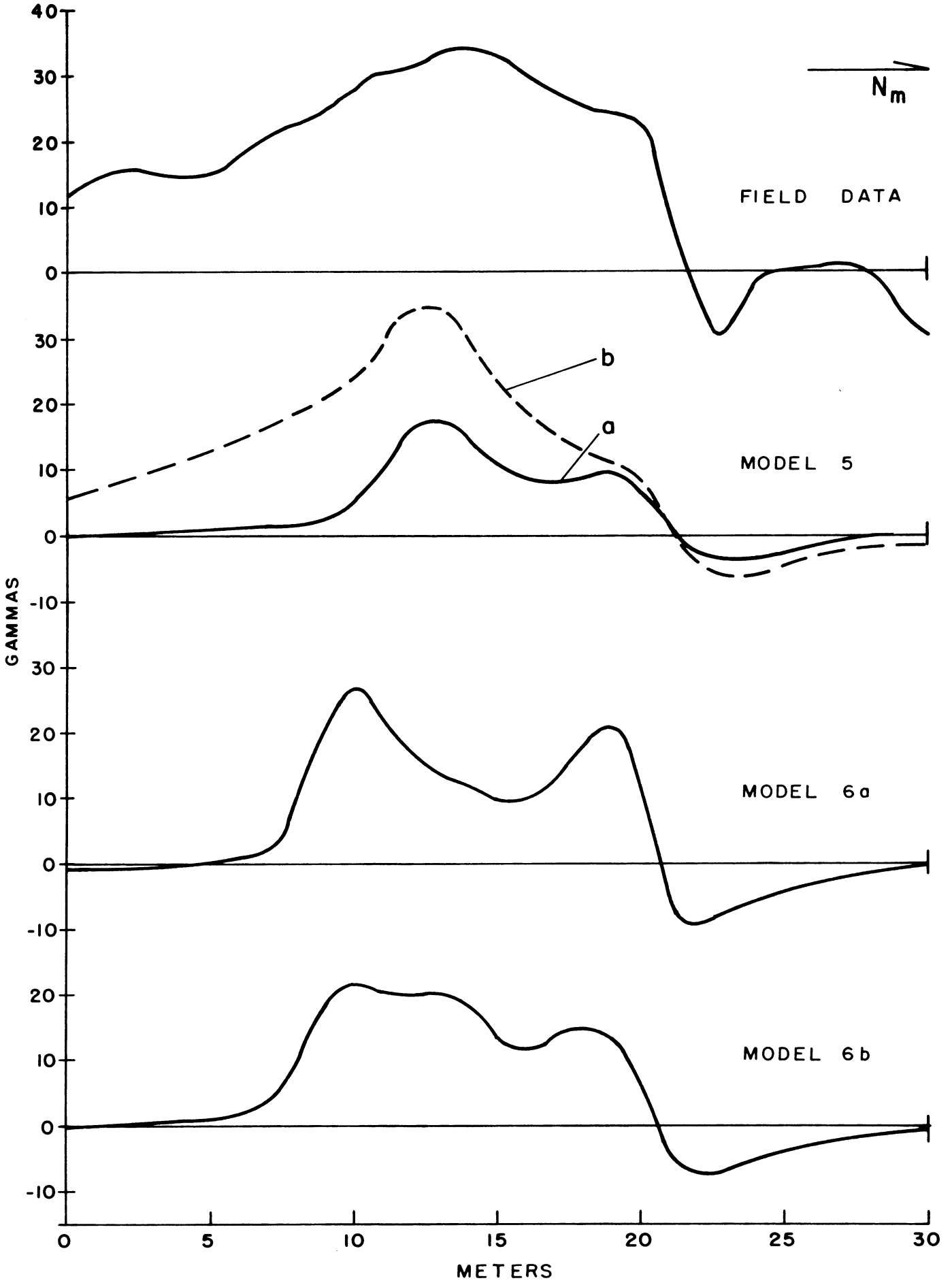


MAGNETIC PROFILES C-C'

Figure 21

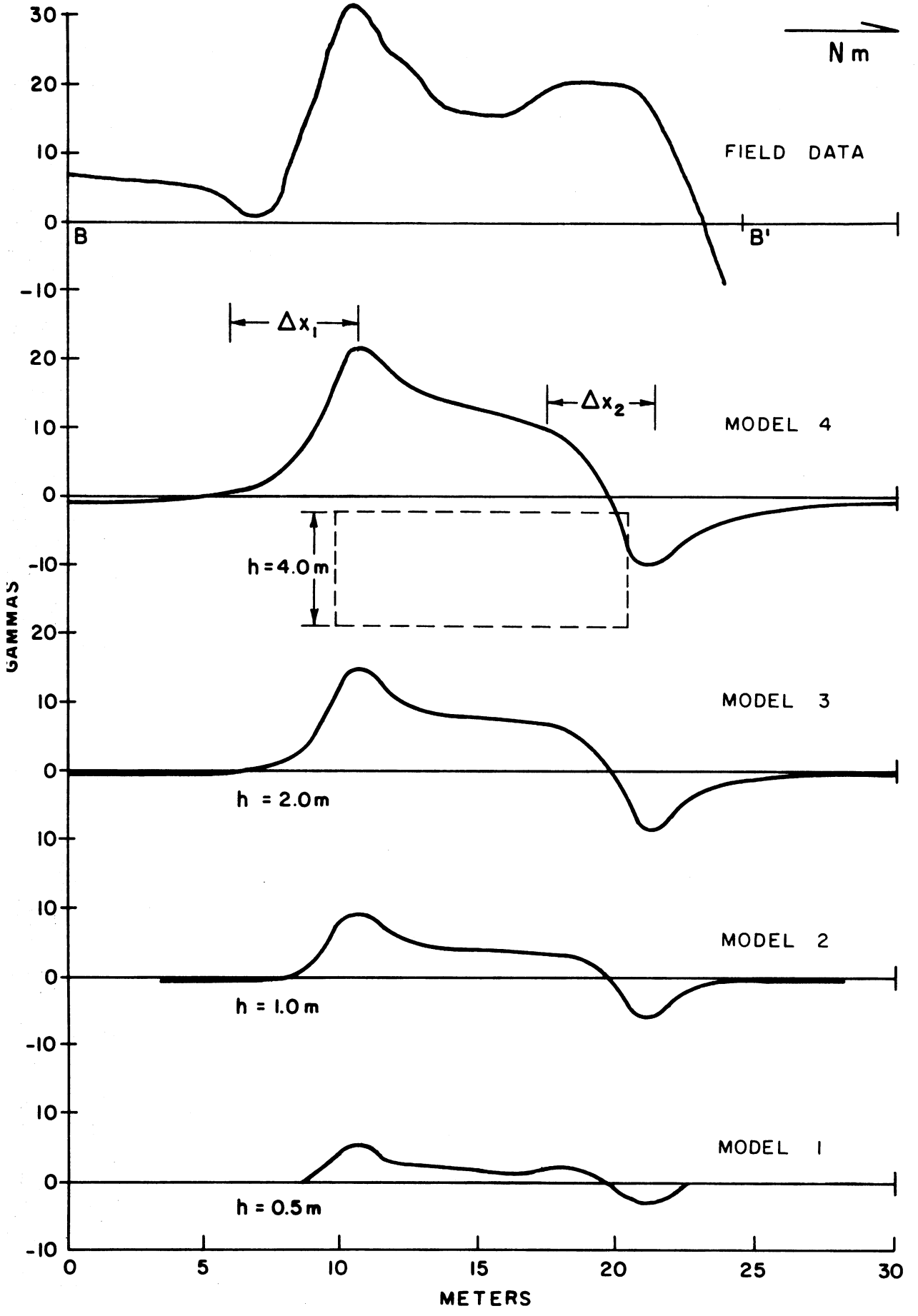


MAGNETIC PROFILES B-B'
SLAB MODELS

Figure 22


PLATE 1

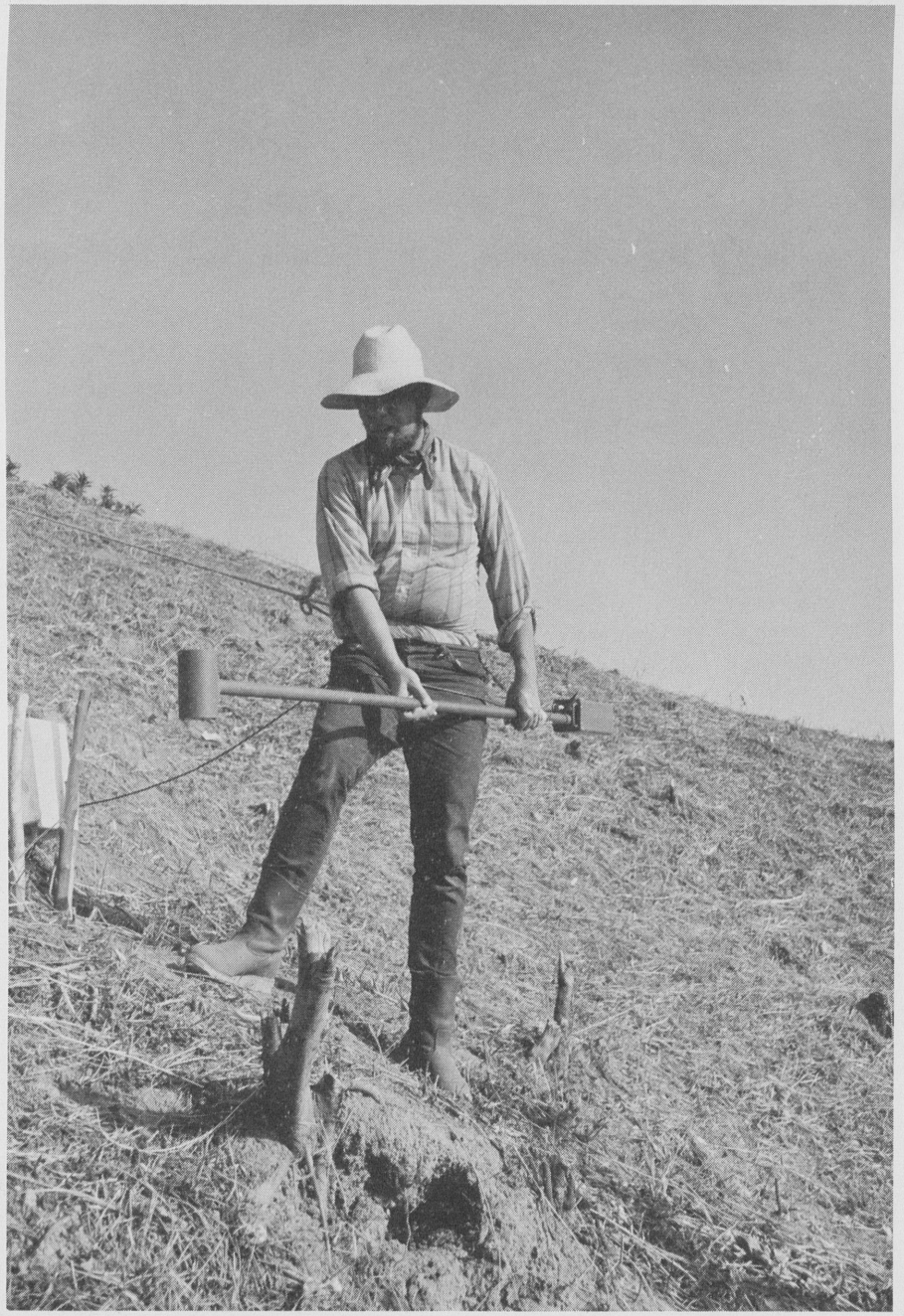

PLATE 2

PLATE 3

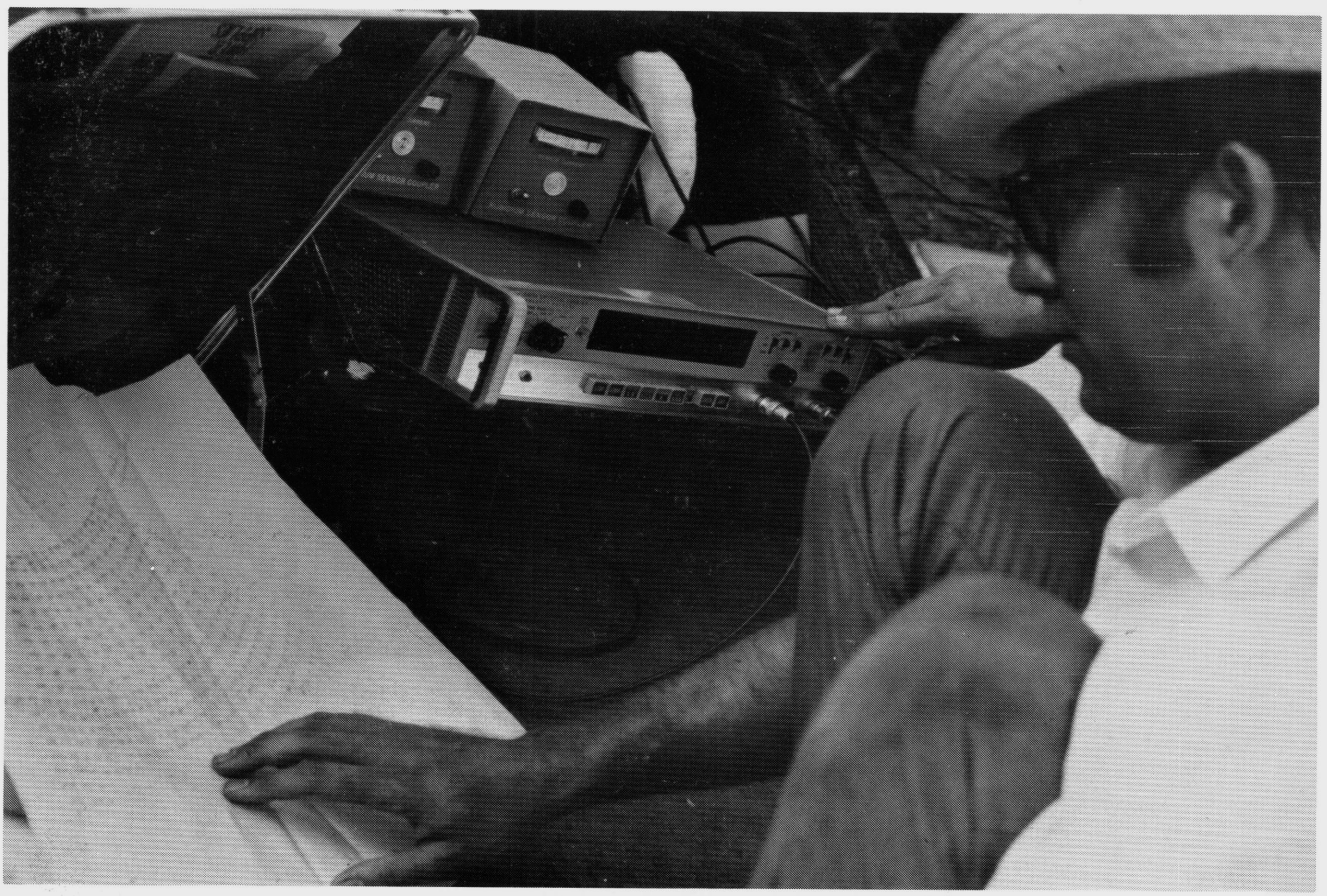

PLATE 4

PLATE 5

PLATE 6

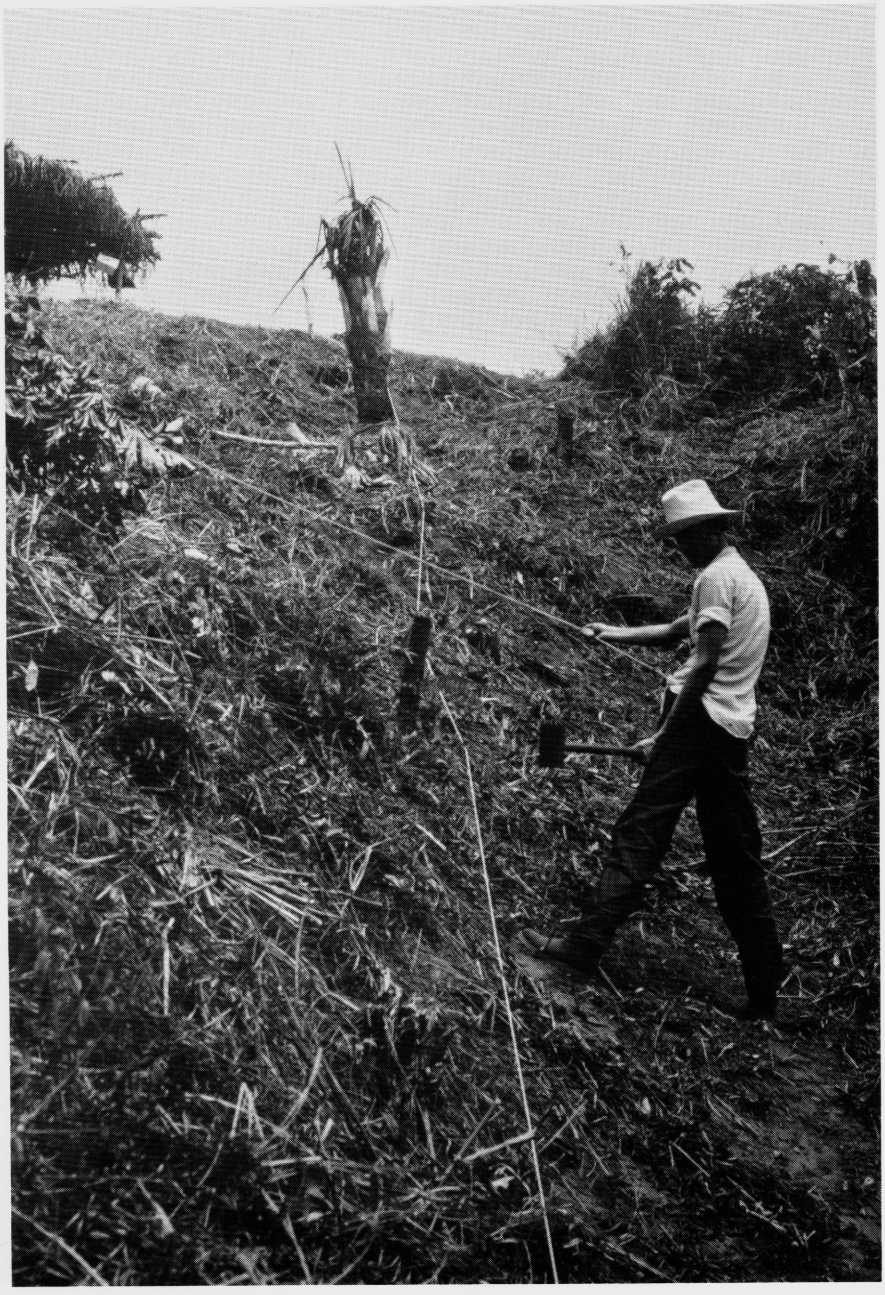

PLATE 7

ROVING SENSOR POSITIONED AT 3 M MARK ON WHITE CORD

# BIBLIOGRAPHY


Aitken, M. J.
1961 Physics and Archaeology. Interscience Publishers, Inc., New York.

Bernal, Ignacio
1969 The Olmec World. University of California Press, Berkeley.

Bhattacharyya, B. K.
1964 Magnetic Anomalies Due To Prisim-Shaped Bodies with Arbitrary Polarization. Geophysics, 29:4:517-531.

Breiner, Sheldon
1965 The Rubidium Magnetometer in Archaeological Exploration. Science, 150:3693:185-193.

Cook, J. C. and S. L. Carts
1962 Magnetic Effect and Properties of Typical Topsoils. Jour. Geophys. Research, 67:815-828.

Drucker, Philip
1952 La Venta, Tabasco: A Study of Olmec Ceramics and Art. Bureau of American Ethnology, Bulletin 153, Washington, D.C.

Drucker, Philip, and Robert F. Heizer
1965 Commentary on W. R. Coe and Robert Stuckenrath's Review of "Excavations at La Venta, Tabasco, 1955". Kroeber Anthropological Society Papers, 33:37-70. Berkeley.

Drucker, Philip, R. F. Heizer, and R. J. Squier
1955 Excavations at La Venta, Tabasco, 1955. Bureau of American Ethnology Bulletin 170, Washington, D.C.

Heizer, R. F.
1968 New Observations on La Venta. Dumbarton Oaks Conference on The Olmec (E. Benson, ed.), 9-40. Washington, D.C.

Heizer, R. F. and P. Drucker
1968 The La Venta Fluted Pyramid. Antiquity, 42:165:75-98. England.

Heizer, R. F., P. Drucker and J. A. Graham
1968 Investigaciones de 1967 y 1968 en La Venta. INAH Boletin, 33:21-28. Mexico.

Heizer, R. F., J. A. Graham, and L. K. Napton
1968 The 1968 Investigations at La Venta. Contributions of the University of California Archaeological Research Facility, No. 5:127-154. Berkeley.

Le Borgne, E.
1955 Susceptibilité magnétique anomale du dol superficiel. Ann. Geophysics, 11:399-419.

Rainey, F., and E. K. Ralph
1966 Archeology and Its New Technology. Science, 153:1481-1491.

Ralph, E. K., F. Morrison and D. P. O'Brien
1968 Archaeological Surveying Utilizing a High-Sensitivity Difference Magnetometer. Geoexploration. 6. (1968), 109-122.

Slichter, L. B.
1942 Magnetic Properties of Rocks. Handbook of Physical Constants, (F. Birch, ed.), Geol. Soc. American Spec. Paper 36, 1942.

Stirling, Matthew W.
1943 Stone Monuments of Southern Mexico. Bureau of American Ethnology Bulletin 138, Washington.

Stuart, G. E. and G. S. Stuart
1969 Discovering Man's Past in the Americas. National Geographic Society, Washington.

Williams, Howel, and R. F. Heizer
1965 Sources of Rocks Used in Olmec Monuments. Contributions of the University of California Archaeological Research Facility, No. 1:1-39. Berkeley.